DR THOMAS L POWELL (Orcid ID : 0000-0002-3516-7164)

DR DANIEL J JOHNSON (Orcid ID : 0000-0002-8585-2143)

Article type : MS - Regular Manuscript

Variation in hydroclimate sustains tropical forest biomass and promotes functional diversity

Thomas L. Powell[1], Charles D. Koven[1], Daniel J. Johnson[2], Boris Faybishenko[1], Rosie A. Fisher[3], Ryan G. Knox[1], Nate G. McDowell[4], Richard Condit[5,6], Stephen P. Hubbell[7], S. Joseph Wright[8], Jeffrey Q. Chambers[1] and Lara M. Kueppers[1,9]

[1]Lawrence Berkeley National Laboratory, Berkeley, CA 94720, USA; [2]Los Alamos National Laboratory, Los Alamos, NM 87545, USA; [3]National Center for Atmospheric Research, Boulder, CO 80305, USA; [4]Pacific Northwest National Laboratory, Richland, WA 99354, USA [5]Field Museum of Natural History, Chicago, IL 60605, USA; [6]Morton Arboretum, Lisle, IL 60532, USA; [7]Department of Ecology and Evolutionary Biology, University of California, Los Angeles, CA 90095, USA; [8]Smithsonian Tropical Research Institute, Apartado Postal, 0843-03092, Panamá, República de Panamá; [9]Energy and Resources Group, University of California, Berkeley, CA 94720, USA

Author for correspondence:
Lara M. Kueppers
Tel: +1 510 486 5813
Email: lmkueppers@berkeley.edu

Received: *2 November 2017*
Accepted: *13 May 2018*

Summary

- The fate of tropical forests under climate change is unclear due, in part, to uncertainty in projected changes in precipitation and in the ability of vegetation models to capture the effects of drought-induced mortality on aboveground biomass (AGB).

- We evaluated the ability of a terrestrial biosphere model with demography and hydrodynamics (Ecosystem Demography, ED2-hydro), to simulate AGB and mortality of four tropical tree plant functional types (PFTs) that operate along light- and water-use axes. Model predictions were compared to observations of canopy trees at Barro Colorado Island, Panama. We then assessed the implications of eight hypothetical precipitation scenarios, including increased annual precipitation, reduced inter-annual variation, El Niño-related droughts, and drier wet or dry seasons on AGB and functional diversity of the model forest.

- When forced with observed meteorology, ED2-hydro predictions capture multiple BCI benchmarks. ED2-hydro predicts AGB will be sustained under lower rainfall via shifts in the functional composition of the forest, except under the drier dry-season scenario.

- These results support the hypothesis that inter-annual variation in mean and seasonal precipitation promotes coexistences of functionally diverse PFTs due to relative differences in mortality rates. If the hydroclimate becomes chronically drier or wetter, functional evenness related to drought-tolerance may decline.

Key words: aboveground biomass, drought, functional diversity, mortality, terrestrial biosphere model, tropical forests.

Introduction

There is considerable variation among climate model projections regarding how precipitation patterns may change over tropical forests over this century (IPCC, 2014). Predictions for the neotropics vary both geographically and by the type of drought, where some regions have general drying, while other regions have a lengthening of the dry season or a reduction in precipitation during either the wet season or dry season (Joetzjer *et al*., 2013; Boisier *et al*., 2015). More frequent El Niño related droughts are also possible for some areas (Li *et al*., 2006; Cai *et al*., 2014). Over parts of Southeast Asia and tropical Africa, however, models predict an increase in total precipitation (IPCC, 2014). Such uncertainty and geographic variation make predicting the fate of tropical forests challenging. Yet, predicting their fate is an extremely high scientific priority because of their importance to the global C cycle and climate system (Bonan, 2008; Pan *et al*., 2011), their exceptionally high species diversity (Dirzo & Raven, 2003), and the precipitation they recycle for agriculture and hydropower (Lima *et al*., 2014; Sumila *et al*., 2017).

In addition to uncertainty surrounding changes in hydroclimate, our understanding of the implications of different drought scenarios on tropical forest C stocks and functional diversity is limited. In particular, it is unclear how 'relative, non-linear' responses of individual trees to environmental variation, which maintains functionally and structurally diverse canopies (Chesson, 2000), buffers tropical forests against changes in hydroclimate. Relative, non-linear responses are the biological responses (e.g. photosynthesis, respiration, C-allocation, xylem cavitation, etc.) individual trees have to fluctuating environmental conditions relative to competing neighbors of differing sizes and plant functional types (PFTs).

The relative, non-linear biological responses to soil water-stress, temperature and humidity of larger trees and drought-intolerant taxa appear to be more acute during severe droughts (Condit *et al*., 1995; Nepstad *et al*., 2007; Meir *et al*., 2015), thus suggesting a significant risk to aboveground C stocks (Rowland *et al*., 2015). However, the net effect of drought-induced mortality on ecosystem C stocks appears to be rapidly offset by ingrowth of

recruits and surviving trees (Fauset *et al*., 2012; Meakem *et al*., 2017). Moreover, less severe droughts or natural long-term climatic drying may cause any elevation in mortality to be more evenly distributed across size-classes or strongest among smaller trees (Fauset *et al*., 2012). Compensatory elevated growth during these brighter, yet drier periods, may help aboveground biomass (AGB) remain stable (Condit *et al*., 2017a). Process-based terrestrial biosphere models that represent the relative, non-linear biological responses to variable precipitation inherent to spatially heterogeneous and diverse forests are a promising tool for synthesizing these observations and assessing the fate of tropical ecosystems across precipitation projections (Levine *et al*., 2016; Weng *et al*., 2015; Zhang *et al*. 2015; Fisher *et al*., 2018).

The Ecosystem Demography model (ED2) is one such tool that simulates light-driven gap-phase dynamics (Moorcroft *et al*., 2001; Medvigy *et al*., 2009), thereby enabling it to characterize present-day spatial and temporal patterns of tropical forest carbon exchange and canopy structure (Powell *et al*., 2013; Zhang *et al*., 2015). Recent incorporation of mechanistic water transport through the soil-plant-atmosphere continuum (ED2-hydro) improves intra- and inter-specific competition for water (Xu *et al*., 2016). ED2-hydro encapsulates the hypothesis that both the relative (in terms of size and PFT), non-linear demographic responses of competing trees to periodic droughts and density-dependent competition for light and water resources are fundamental regulators of tropical forest AGB and functional diversity. However, ED2-hydro (and other terrestrial biosphere models with hydrodynamics) still requires further evaluation of its ability to capture diverse drought responses in order to build confidence in its predictions of tropical forest vulnerability to droughts. In particular, mortality dynamics that arise from size- and density-dependent competition for light and water still remain largely untested in ED2-hydro and terrestrial biosphere models in general. The Smithsonian Institution's 50-ha monitoring plot at Barro Colorado Island (BCI), Panama, is a rigorous test case for evaluating predictions of AGB, mortality and functional diversity by ED2-hydro. Detailed measurements of trees >1 cm diameter at breast height (dbh) have been made in the plot regularly from 1982 to the present (Condit, 1998), a period that includes three major El Niño droughts (Condit *et al*., 1995, 2017) and an unusually wet year.

Our overarching goal is to understand the risk that projected changes in global hydroclimate pose for tropical forest C stocks and function. We first confronted ED2-hydro mortality and AGB predictions with observations from BCI. Second, we simulated six idealized

drought scenarios and two increased precipitation scenarios, all based on climate model predictions, to examine the response of moist evergreen tropical forest AGB and functional diversity. Finally, we conducted a cross-scenario analysis to gain insight into emergent relationships between modeled drought responses and soil moisture.

Materials and Methods

Study site

The 50-ha long-term forest monitoring plot on Barro Island Colorado (BCI) in central Panama (9.151ºN, 79.855ºW) was the test case for this analysis. BCI supports a moist evergreen tropical forest with mean annual precipitation of 2662±479 (SD) mm yr^{-1} (Fig. 1) and a 4-month dry season (<100 mm per month) (Fig. 2a). The forest is predominantly evergreen: only 10% of the canopy fraction drops leaves during the dry season (Condit *et al*., 2000). After establishment in 1981, the species and dbh of all living trees >1 cm have been systematically inventoried every 5 yr since 1985 (Condit, 1998). Data from these inventories are the basis for the benchmarks described below.

ED2-hydro model and parameterization

The Ecosystem Demography model version 2 with hydrodynamics (ED2-hydro; Medvigy *et al*., 2009; Xu *et al*., 2016) is a state-of-the-art terrestrial biosphere model that simulates fast time-scale physiological and biogeochemical processes with closed carbon and energy budgets. Except where noted below, this ED2-hydro tropical forest parameterization follows Powell *et al*. (2013) (ED2, version 2.1rv76) for leaf, stem and root physiology, canopy biophysics, carbon allocation, and soil physics (see also Moorcroft *et al*., 2001; Medvigy *et al*., 2009), and follows Powell (2015) for plant hydraulics and stomatal regulation (see also Xu *et al*., 2016). In short, ED2-hydro uses a size-, age-, and strategy-structure to track the demographic rates of ensembles of individuals, called cohorts, growing together in spatially implicit 'patches' of different ages since their last disturbance. Each patch has different structural and physical characteristics that together represent a mosaic of vertically and horizontally stratified competition for light and water resources (Levine *et al*., 2016).

All cohorts belong to one of four tropical tree PFTs, each parameterized to represent a particular competitive strategy. The four PFTs simulated in this study were:

1. early-successional drought-tolerant,
2. early-successional drought-intolerant,
3. late-successional drought-tolerant and,
4. late-successional drought-intolerant.

In tropical forests, trees with lower wood density (ρ_{wood}) have, on average, higher relative growth rates in high light and higher mortality rates in low light compared to trees with higher ρ_{wood} (Muller-Landau, 2004; King *et al*., 2006; Poorter *et al*., 2010; Wright *et al*., 2010). Consistent with this, ED2-hydro assumes early- and late-successional PFTs differ in their intrinsic photosynthetic and transpiration rates, parameterized through differences in maximum stem hydraulic conductivities ($K_{s,sat}$) (see later), maximum carboxylation rates and stomatal slopes (Powell, 2015; Powell *et al*., 2013) and through differences in background mortality rates as a function of ρ_{wood} (Moorcroft *et al*., 2001) (Table 1). Wood density was prescribed as 0.40 and 0.68 g cm^{-3} for early- and late-successional PFTs, respectively. The observed range of ρ_{wood} for canopy species is 0.32 to 0.84 g cm^{-3} (Wright *et al*., 2010). The mortality algorithm follows the original ED model (Moorcroft *et al*., 2001), but uses parameters specific to this study (Table 1). The model prescribes fixed, PFT-specific background mortality rates ($mortality_{bg}(PFT)$) of 0.055 and 0.014 yr^{-1} for early- and late-successional PFTs, respectively (Table 1). Cohorts can also experience an additional, negative C-balance mortality ($mortality_{cb}$) that emerges from dynamic physiological responses to density-dependent competition for light and water (Table 1). Background mortality encompasses all modes of mortality not explicitly accounted for through $mortality_{cb}$. Stomatal regulation, in particular, can lead to elevated $mortaltiy_{cb}$ during vapor pressure (Medvigy *et al*., 2009) and soil moisture (Powell, 2015, described below) deficits, where the latter is caused by low precipitation and density- and size-dependent water-use. Mortality associated with successional type (background and light-limitation) is largely independent of mortality associated with drought-tolerance (soil moisture limitation) (Christoffersen *et al*., 2016; Powell *et al*., 2017), as ρ_{wood} is not correlated with the hydraulic traits (except $K_{s,sat}$, see later) (Table 1), except that both types of mortality are sensitive to number-density.

Reproduction follows the original ED parameterization (Moorcroft *et al*., 2001). All PFTs convert a set fraction (0.3) of positive net carbon production to new recruits. Therefore, the model assumes that water and light availability do not affect seedling survivorship to 1 m—the initial height for new recruits.

The drought-tolerant and -intolerant PFTs are defined by a hydrodynamic parameterization that tracks water potential through the soil-plant-atmosphere continuum (Williams *et al*., 1996, 2001; Xu *et al*., 2016). The formulation represents hydraulic conductivity of the soil and stem, xylem vulnerability to cavitation, capacitance, and stomatal sensitivity to leaf water potential. Parameter values for each are given in Table 1. The Xu *et al.* (2016) hydrodynamics formula was adapted here to represent drought-tolerance (but not drought-avoidance as in Xu *et al.* (2016)) as a strategy between PFTs (Powell, 2015). The drought-tolerant and -intolerant PFTs differ in their $K_{s,sat}$ values, and two-parameter Weibull cumulative distribution functions (Bohrer *et al*., 2005) that represent xylem vulnerability to cavitation and stomatal sensitivity to leaf water pressure (Powell, 2015) (Table 1). The Weibull functions, which control cohort-level 'relative, non-linear responses' to changes in soil moisture, were parameterized to pass through PFT-specific stomatal and xylem P_{50}'s—i.e. the point where conductance equals 50% of its maximum (Table 1). Stomatal P_{50} values were assumed to equal leaf turgor loss points (Brodribb *et al*., 2003). Turgor loss points and xylem P_{50}'s (Table 1) were obtained from direct measurements of Amazonian species (Powell *et al*., 2017). In the hydrodynamic formulation, the Weibull functions range from 0 to 1 and either constrain water supply to the leaf or down-regulate leaf photosynthesis and transpiration as soil water content decreases (Powell, 2015).

Stem capacitance was set to 204 kg-H_2O m^{-3} MPa $^{-1}$ across all PFTs, which is within the observed range of tropical species with our selected wood densities (Meinzer *et al*., 2003; Carrasco *et al*., 2015). $K_{s,sat}$ was tuned *a priori* to the BCI benchmarking analysis (described below) to first, produce coexistence of the four PFTs, second have the late-successional PFTs comprise approximately two-thirds of AGB, and third, have the AGB of the drought-tolerant and -intolerant PFTs in equal proportions when rooting depth equals 3 m. The successional-type proportions are based on the observation that BCI is largely comprised of 'generalists' (late-successional) compared to 'pioneers' (early-successional) (Condit *et al*., 1995). Early-

successional PFTs were given higher $K_{s,sat}$ values than late-successional PFTs (Campanello *et al*., 2008) to facilitate higher growth rates via higher water supply to the leaf.

For all PFTs, maximum tree heights and rooting depths were set to 38 m and 3 m, respectively. Root biomass follows a power function truncated at 3m (Table 1). The soil hydraulic properties follow Clapp & Hornberger (1978). Soil textures (70% clay, 10% sand, 20% silt) are from observations of the top 2.5 m of the upland forest soil at BCI (Ben Turner, personal communication). All model simulations were of the slopes and upland portions (47.5 ha) of the BCI monitoring plot (a seasonal swamp was excluded). Modeled soil moisture does not transfer between patches since adjacent, but structurally different, tropical forest patches can have contrasting soil moisture profiles (Miller *et al*., 2011). Thus, the simulated patches have explicitly different light and water environments across the successional gradient. A 5-m rooting parameterization was also tested to evaluate the sensitivity of model predictions and the robustness of our conclusions when available soil water is increased.

Model benchmarking

Previous studies have shown that ED2 can credibly predict carbon fluxes and AGB of tropical forests under current climate (Powell *et al*., 2013; Knox *et al*., 2015; Zhang *et al*., 2015; Levine *et al*., 2016) and capture water fluxes and leaf area dynamics of a seasonally dry tropical forest (Xu *et al*., 2016). This study evaluates ED2-hydro simulations of total ecosystem AGB, stand structure, and mortality rates, which have not previously been evaluated, for BCI upland forests.

ED2-hydro was forced using hourly measurements of local meteorology obtained between 2008 and 2014 (Powell *et al*., 2018). The meteorology QA/QC protocol involved removing spurious data, step-changes, and sensor-drift trends and then statistically gap-filling missing data. Short-wave radiation, wind speed, atmospheric pressure, air temperature and relative humidity were measured above the canopy. Precipitation was measured in an opening adjacent to the 50-ha plot. Short wave radiation was split into four components: direct visible (29.2%), direct near-IR (38.8%), diffuse visible (16.6%) and diffuse near-IR (15.4%) (Goudriaan, 1977). Atmospheric CO_2 was held constant at 385 ppm for all simulations.

A potential forest was spun up for 700 yr from a near-bare-ground initialization using repeated cycles of the meteorological data until total AGB, stand size-structure and soil carbon

pools reached equilibrium. The 700th year of the spin-up was used to initialize all benchmarking and precipitation scenario simulations.

Model predictions from the 300th year of the baseline precipitation simulations (BASE, see later) were compared to total ecosystem AGB from the 1985 to 2000 inventories of the 50-ha plot (Chave *et al*., 2003) and basal area and mortality size-class distributions from the 2005 and the 2005 to 2010 censuses, respectively (data source: Condit *et al*., 2012a; data mortality equations: Condit *et al*., 2017a). Because the model does not simulate understory specialists (i.e., all PFTs can attain a maximum height of 38 m), the inventory data were first screened to only include 'canopy' species—i.e. species having at least one measured individual >20 cm dbh (Supporting Information Fig. S1). For the size-class distribution comparisons, data were binned by 10 cm dbh classes and partitioned by ρ_{wood} into early-successional (<0.49 g cm^{-3}) and late-successional (≥0.49 g cm^{-3}) groups. The tree species observed at BCI were also binned into quartiles along the relative growth rate versus mortality continuum (Wright *et al*., 2010), with mean (±standard error) mortality and ρ_{wood} values calculated for each quartile. The alignment of the observed ρ_{wood} versus mortality continuum was compared to that of the model to assess both our *a priori* use of 0.40 and 0.68 g cm^{-3} for ρ_{wood} of the early- and late-successional PFTs, respectively, and the general applicability of the mortality algorithm (Table 1) to BCI.

Drought sensitivity simulations

We ran eight precipitation experiments plus the BASE scenario as a control (Table 2; Notes S1, S2). The primary analysis using a 3 m rooting depth and the sensitivity analysis using a 5 m rooting depth followed the same protocol. The BASE scenario was simply a continuation of the spin-up. Annual (Fig. 1) and mean monthly (Fig. 2a) precipitation for the BASE scenario reasonably represents the precipitation patterns in the long-term observations (1930–2014). All scenarios used months drawn from the BASE meteorology in order to retain as much natural structure (i.e., diel to seasonal variation) and covariation among variables as possible.

The average scenario (AVG) is a composite of 12 months selected from 2008 to 2014 that are nearest to the long-term mean precipitation for that month, thereby retaining seasonality but removing inter-annual variation (Fig. 2b). The longer dry season scenarios extend the dry season of the AVG scenario by three months (6 wk at the beginning and end) every year (DRY1) (Fig. 2b), every other year (DRY2), and every 3rd year (DRY3). For DRY-WS, BASE wet

season (May to December) precipitation is reduced by 40% (one standard deviation below the long-term mean). For DRY-DS, BASE dry season precipitation (Jan. to Apr.) is reduced by 75%, which reflects the most extreme dry season droughts observed from 1930 to 2014. WET persistently increases annual precipitation by 30% by using only 2010 and 2011 of the BASE meteorology. The effects of extreme El Niño-related droughts were simulated by inserting into the BASE recycled loop once every 20 yr (the approximate occurrence at BCI, e.g. 1982–1983, 1997, 2016) a synthetically derived El Niño meteorology based on the observed precipitation at BCI from the 1982/83 El Niño (SYN-ENSO) (Fig. 2c, S2, S3; Notes S2; Table S1). Adjacent dry days were substituted for days with precipitation in the extended dry season (DRY1, DRY2, and DRY3) and El Niño (SYN-ENSO) drought scenarios, thus resulting in higher than average radiation and lower than average humidity during the drought periods in those scenarios, which we assumed is generally the case for these types of droughts. By contrast, only precipitation was manipulated in the DRY-WS and DRY-DS scenarios.

Analysis

We used plant available soil water (PAW) as an explanatory variable for predicting the relationship between forest functional diversity and water availability. PAW was calculated as the difference between the simulated total soil water content (mm) through the rooting zone and soil water content at the wilting point (-1.5 MPa). Canopy throughfall (i.e., precipitation minus canopy interception) was the upper soil layer input.

We calculated a metric of selection for drought-tolerant functional strategies (the drought tolerance ratio) as the ratio of AGB of the drought-tolerant PFTs to total AGB, where a value of one indicates complete dominance by drought-tolerant PFTs, and zero indicates dominance by drought-intolerant PFTs:

$$drought\ tolerance\ ratio = \frac{AGB\ drought\ tolerant\ PFTs}{Total\ ecosystem\ AGB}. \qquad \text{Eqn 1}$$

The Shannon-Wiener evenness index (E) was calculated as an index of total functional diversity of the ecosystem:

$$E = \frac{H}{\ln(S)} \quad \text{Eqn 2(a)}$$

$$H = \sum[P_i \times \ln(P_i)]. \quad \text{Eqn 2(b)}$$

H is the Shannon-Wiener diversity index, *S* is PFT richness (four in all cases), and *P* is the proportion of total AGB comprised of PFT *i*. Values of *E* range from zero to one, where zero represents complete dominance by a single PFT and one represents equal proportions of all PFTs.

The source code, parameterization files and meteorological forcings used in this study are available in Notes S3 and S4.

Results

Model evaluation

The performance of the ED2-hydro parameterization was evaluated in five ways: (1) AGB predictions, (2) establishment and coexistence of PFTs that compete along light and water resource axes, (3) ecosystem and PFT level mortality dynamics during normal and drought years, (4) size-class distributions of basal area and mortality rates, and (5) validity of the assumed relationship between ρ_{wood} and mortality. Under baseline meteorology, ED2-hydro predicts the equilibrium AGB to be 13.5 kg C m^{-2}, which agrees with an inventory-based estimate of 14.0 ± 1.0 kg C m^{-2} for 1985–2000 (Chave *et al.*, 2003) (Fig. 3). The model predicts that the four PFTs come into coexistence and reach a dynamic equilibrium after *c*. 300 yr with the late-successional PFTs jointly comprising approximately two-thirds of AGB (Fig. 3). As expected, the early-successional PFTs are first to colonize bare ground or newly formed gaps (Fig. S4); but the drought-tolerant PFTs (both early- and late-successional) dominate the next 150 yr (Fig. 3). Drought-tolerant PFTs dominate early because ED2-hydro initializes patches with a very high density of recruits (data not shown), which when coupled with their shallow roots, quickly leads to water-stress during the initial stages of patch development. Once all of the PFTs occupy their equilibrium space, the AGBs of drought-tolerant and -intolerant PFTs are anti-correlated (i.e. years 300–1000 in Fig. 3). Although coexistence of the four PFTs was, in part, achieved through tuning $K_{s,sat}$, before this study it was unclear if coexistence would occur and hence, it is a significant result. Also, the order of PFT establishment, time to equilibrium, and the chaotically-

fluctuating anti-correlation of drought-tolerant and -intolerant PFTs (Fig. 3) emerge from the internal dynamics (i.e. physiological and demographic functions) of the model.

Predicted mortality dynamics were evaluated using the SYN-ENSO precipitation scenario because the first set of forest observations in the time series includes the 1982/83 El Niño. Mortality dynamics for the non-El Niño years in the SYN-ENSO scenario are similar to the mortality dynamics in the BASE scenario. A selected 30-yr period from the SYN-ENSO precipitation scenario shows that whole ecosystem mortality for trees >10 cm dbh ranges between 3.3% yr^{-1} in relatively wet years to 6.8% yr^{-1} in relatively dry years and reaches as high as 10.0% in El Niño drought years (Fig. 4a). The lower range of the mortality predictions agrees well with the observed range of mortality rates for canopy trees (Fig. 4a) (Condit *et al*., 2012a). Modeled mortality rates of the early-successional trees are more than double that of the late-successional trees, and they are considerably more responsive to precipitation dynamics (Fig. 4b). Because early-successional trees have higher intrinsic transpiration rates compared to late-successional trees, their leaf water potentials drop more quickly during dry periods, which leads to stomatal closure and cavitation, and ultimately drives $mortality_{cb}$ higher (Table 1). Modeled mortality of both the early- and late-successional PFTs markedly increased during the simulated El Niño droughts (Fig. 4b). The mortality dynamics that emerge between wet and dry years create sufficient niche space for each PFT to periodically outcompete its drought-tolerant or -intolerant counterpart (Fig. 4c). This reflects the hypothesized trade-off between growth and drought-tolerance parameterized though the hydrodynamic and mortality functions in the model. As expected, predicted mortality rates of the late-successional drought-intolerant PFT are always higher than those of the late-successional drought-tolerant PFT during the El Niño droughts. By contrast, predicted mortality rates of the early-successional drought-intolerant PFT are only sometimes higher than the early-successional drought-tolerant PFT during El Niño droughts (Fig. 4c).

The model captures the right-skewed basal area size-class distribution of early-successional, late-successional and all canopy trees at BCI (Fig. 5a–c). The model also partitions the basal area distributions in correct proportions between the early- and late-successional PFTs as compared to observations, thus supporting the predictions of the relative distributions of AGB (Fig. 3b). Two notable exceptions to the strong agreement are in the largest size-class (trees >100 cm dbh) of the early-successional PFT (Fig. 5a) and the two smallest size-classes (trees

<20 cm dbh) of the late-successional PFT (Fig. 5b). In the case of the former, the model fails to capture the observed occurrence of very large, but relatively rare, canopy emergent light-demanding species (examples: *Ceiba pentandra* (L.) Gaertn., *Dipteryx oleifera* Benth.; taxonomic source: Condit *et al*., (2017b); S. J. Wright, pers. obs.).

The model over-estimates canopy-tree mortality rates across all size-classes for the early-successional PFTs, with the greatest deviations between model predictions and observations occurring in the smallest size-classes (Fig. 5d). The excessively high bias in mortality rates of the smaller size-classes cancels out a high bias in recruitment rates for the early-successional PFTs; hence the basal area distribution is of the correct magnitude in all size-classes below 90 cm dbh (Fig. 5a). On the other hand, the high bias in mortality rates of the largest size-class prevents the model from capturing the aforementioned large early-successional canopy-emergent trees.

With the exception of the smallest trees (<10 cm dbh), model predictions agree with the observed size-class distribution of mortality rates for the late-successional trees (Fig. 5e). When aggregated to the ecosystem, model predictions agree with observations in the intermediate size-classes, but overestimate mortality rates for the smallest and largest sized trees (Fig. 5f). This overestimation is accounted for by the early-successional PFTs (Fig. 5d).

Predicted total mortality rates (i.e. $mortality_{bg}$ + $mortality_{cb}$, Table 1) of the early- and late-successional PFTs are aligned with the observed ρ_{wood} versus mortality continuum for species at BCI (Wright *et al*., 2010) (Fig. 6), noting that both observed and modeled mortality include all modes. The model alignment with the observed continuum indicates that the four mortality parameters (Table 1) are of the correct magnitude. The ρ_{wood} and predicted mortality rates of the late-successional PFTs agree strongly with the data quartile most analogous to them on the observed continuum, thus supporting our prescribed ρ_{wood} (0.68 g cm^{-3}). By contrast, predicted mortality of the early-successional PFTs is at the extreme upper end of the continuum and beyond the standard error of their most analogous data quartile, thus indicating that the ρ_{wood} prescribed to the early-successional PFTs (0.40 g cm^{-3}) may be too low.

Model projections of AGB under different drought scenarios

ED2-hydro predicts that the long-term AGB dynamics of the individual PFTs will respond differently to alternative future hydroclimates (Fig. 7). For the SYN-ENSO and DRY3 (Fig. S5)

scenarios, the AGB dynamics of the four PFTs remain similar to the BASE scenario (Figs 7a,d). The AVG and WET scenarios result in a significant increase in AGB of drought-intolerant PFTs with a commensurate decrease in the drought-tolerant PFTs (Fig. 7b,c). By contrast, the DRY-WS, DRY-DS and DRY1 scenarios result in an almost complete loss of the drought-intolerant PFTs, with a commensurate increase in the drought-tolerant PFTs (Fig. 7e–g). Similarly, a loss in AGB of the drought-intolerant PFTs and increase in the drought-tolerant PFTs occur under the DRY2 scenario, but are comparatively smaller in magnitude (Fig. 7h).

ED2-hydro predicts that the long-term equilibrium of total ecosystem AGB remains within the current observed range for all precipitation scenarios except the more severe dry season scenario, DRY-DS (Fig. 7i). Under DRY-DS, the model predicts equilibrium AGB of the ecosystem (12.0 kg C m^{-2}) will decline by 11% compared to the baseline scenario (BASE) and c. 15% compared to observations (Fig. 7i). By contrast, the model predicts equilibrium ecosystem AGB is highest under the AVG scenario (14.5 kg C m^{-2}) (Fig. 7i, upper grey line).

Equilibrium total AGB across precipitation scenarios is largely controlled by the long-term (i.e. > 10 yr) mean state of PAW in the late dry season (i.e. March and April, Fig. 8); whereas AGB is poorly related to mean annual PAW (Fig. S6). The model also predicts that the ratio of drought-tolerant PFTs to drought-intolerant PFTs of moist evergreen tropical forests similar to BCI is controlled by the mean annual state of PAW (Fig. 9a), not the severity of the dry season as for total AGB (Fig. 8). For example, the precipitation scenarios AVG and WET resulted in relatively high mean annual PAW values and drought-intolerant PFTs accounted for >70% of AGB, whereas drought-intolerant PFTs accounted for <20% of AGB in the DRY1, DRY-WS, and DRY-DS scenarios (Fig. 9a). Interestingly, only the late-successional PFTs were affected by the AVG scenario, while all four PFTs were affected by the WET scenario (Fig. 7b,c).

The Shannon-Wiener evenness index showed that functional diversity in moist evergreen tropical forests is strongly controlled by the mean annual state (i.e., for periods > 10 yr) of PAW (Fig. 9b). An intermediate level of drought frequency (e.g., BASE, SYN-ENSO, DRY2 and DRY3 precipitation scenarios) promotes the highest level of functional diversity of the four PFTs (Fig. 9b). By contrast, scenarios with more rain and less inter-annual variation (AVG, WET), or with very frequent droughts (DRY1, DRY-WS, DRY-DS) leads to reductions in evenness across the four PFTs (Fig. 9b).

Model predictions are not qualitatively different when PAW is increased by changing the maximum rooting depth to 5 m (Notes S5; Fig. S7–S10).

Discussion

We evaluated the predictive ability of ED2-hydro to capture forest structure and dynamics of functionally distinct trees within a moist evergreen tropical forest; and examined the effects of various manifestations of drought on functional diversity and aboveground C stocks.
Our benchmarking analysis demonstrated that coexistence of four PFTs competing directly for light and water resources is achievable within a terrestrial biosphere model formulated with a density-, size-, and strategy- (i.e. PFT) dependent structure. The model also produces credible predictions of AGB and mortality. Coexistence of the four simulated PFTs occurs as a result of the intersection between the modeled non-linear biological responses and variation in precipitation, which creates a multidimensional niche space across the simulated gaps that comprise the forest mosaic. From the drought scenario analysis, we demonstrated that: 1) variation in precipitation, and thereby PAW, regulates functional diversity in this model structure, 2) most drought scenarios lead to shifts in functional diversity without a reduction in AGB, and 3) only a shift towards a more severe dry season leads to a reduction in both functional diversity and AGB. Therefore, we propose that environmental factors controlling total AGB differ from those controlling functional diversity, due in part to the relative, non-linear, biological responses to drought by differing PFTs that lead to compensating growth and mortality.

Model formulation and benchmarking

ED2-hydro is a state-of-the-art terrestrial biosphere model (Fisher *et al*., 2018) that explicitly represents density-, size- and PFT-dependent processes hypothesized to govern AGB and coexistence in tropical forests (Chesson, 2000; Levine *et al*., 2016). ED2-hydro has performed well against benchmarks from a seasonally dry tropical forest in Costa Rica (Xu *et al*., 2016) and three different moist tropical forests, one in BCI (this study) and two in the eastern Amazon (Powell, 2015), which supports its application here. Notably, the soil and meteorological boundary conditions used in this study are from BCI; but, the biological parameterization is

largely based on tropical forest meta-analyses or studies from Amazonian tropical forests (Moorcroft *et al*., 2001, Powell *et al*., 2013). Only the ρ_{wood} and $K_{s,sat}$ parameters were tuned in this study before benchmarking. The agreement between model predictions and observed BCI benchmarks (Figs 3, 4a, 5) implies that the ED2-hydro hypotheses related to density-, size-, and PFT-dependence generalize across moist evergreen tropical forests with similar soil properties as BCI and are important ecological processes to include in terrestrial biosphere models when assessing drought effects on tropical forests. Our results specifically indicate that models formulated as such can largely capture both mortality of moist evergreen tropical forests (Figs 4a, 5d–f) and niche partitioning between PFTs that is created by differential mortality rates under variable precipitation (Fig. 4c).

Observed size-distributions are critical benchmarks for size structured model to ensure they correctly account for non-linear size-dependent physiological and demographic responses. The over-estimation of basal area and mortality in the smaller size-classes (Fig. 5c,f) predicted by ED2-hydro is understood: it is caused by a poorly constrained transfer of C to tree recruitment (Moorcroft *et al*., 2001) that results in the number-density of new recruits being too high. This problem arises from a compromise that enables ED2-hydro to satisfy a fundamental condition of terrestrial biosphere models: they must conserve carbon and energy in order to serve as a lower boundary for Earth System Models. This compromise does not preclude ED2-hydro from being informative for drought analyses such as ours because it makes robust predictions of biomass and mortality in size-classes >30 cm dbh, which account for the preponderance of ecosystem biomass and function (Meakem *et al*., 2017). Future work on the representation of C-allocation and recruitment should aim to diminish this bias.

The ED2-hydro parameterization largely captures the fast-slow axis of competition characteristic of successional dynamics (Reich, 2014) where the early-successional PFTs colonize high-light environments first (Fig. S4), but eventually become less dominant (Fig. 3) due to higher mortality rates of mature trees and recruits growing in the understory (Figs 4b, 5d,e). The higher mortality rates of the early-successional PFTs are, in part, directly parameterized through a phenomenological relationship with ρ_{wood} (Table 1). The mortality calculation also represents carbon starvation resulting from competition for light and water with other individuals sharing a patch, thus yielding dynamic mortality above the fixed background rates of 0.055 and 0.014 yr^{-1} of the early- and late-successional PFTs, respectively (Fig. 4b). The

ED2-hydro approach of making C-balance mortality additive to PFT-dependent background mortality (Table 1) is supported by the strong alignment between the BCI observations (Wright *et al*., 2010) and model predictions of total mortality for early- and late-successional PFTs vs ρ_{wood} (Fig. 6).

In terms of drought, per capita use of PAW is not just a function of the PAW pool. Rather, per capita use of PAW is also a function of the characteristics of the individuals (number, size, and type) drawing on the PAW pool (Young *et al*., 2017), which in turn sets a cardinal constraint on the carrying capacity of trees in the forest. Many terrestrial biosphere models use alternative approaches for representing mortality that, for example, either apply a single turnover rate to total ecosystem NPP or biomass (Galbraith *et al*., 2013) or spatially scale turnover to a prescribed gradient (Castanho *et al*., 2013), but they do not explicitly account for density-dependent mortality related to light limitation or PAW. These alternative hypotheses about the ecological controls over mortality have had limited success in reproducing tropical forest drought responses (Powell *et al*., 2013). Our benchmarking results lend support for including density-dependent mortality in terrestrial biosphere models used to simulate drought responses.

Coexistence and climatic variability

Sakschewski *et al*., (2016) recently demonstrated with a terrestrial biosphere model that functional diversity in tropical forests confers resilience to climate change because it increases the number of combinations in strategies that infill newly created niche space. Our parameterization of ED2-hydro is consistent with this conclusion in that it includes functional diversity in both light and water resource dimensions compared to the light-only dimension of the original ED2 model (Medvigy *et al*., 2009), which struggled to capture experimental drought responses observed in the Amazon rainforest (Powell *et al*., 2013). Our results, however, differ from Sakchewski *et al*. (2016) in one interesting way: here resilience is predicted with relatively few PFTs, and hence, trait axes. This difference may arise from the explicit representation of plant hydrodynamics and its interaction with successional dynamics in our study, which was not explicitly considered in Sakschewki *et al.* (2016). In highly diverse tropical forests, species certainly array along functional continua (Fig. 6), such as early- vs late-successional (e.g. King *et al*., 2006; Wright *et al*., 2010) and drought-tolerant versus –intolerant (e.g., da Costa *et al*., 2010; Condit *et al*., 2013). ED2-hydro's success in reproducing the benchmarks (Figs 3, 4a, 5, 6) and

simulating reasonable mortality dynamics (Fig. 4c) suggests that the trade-offs associated with light and water acquisition in highly diverse forests can collapse into relatively few functional groups and still capture drought responses in hypothetical precipitation scenarios (see also Sterk *et al*., 2011).

The role of climatic variability in promoting coexistence and functional diversity in old growth tropical forests has been difficult to demonstrate empirically because we lack monitoring plots that cover sufficiently-long temporal scales (Clark *et al*., 2017). Our benchmarking analysis demonstrates that ED2-hydro is suitable for exploring how different manifestations of drought regulate coexistence and alter functional diversity in tropical forests. The independent patch structure of the model leads to a range of soil moisture environments and hence, facilitates coexistence. It is, however, unclear how predicted changes in coexistence may be modified by a patch structure that retains independent light environments but greater soil moisture connectivity across the successional gradient. Also, many other processes aside from variation in precipitation likely play an important role in the maintenance of tropical forest diversity (Wright *et al*., 2002; Condit *et al*. 2012b); but they are beyond the scope of this analysis.

A key result from this modeling study is that the precipitation scenarios containing high intern-annual variation – e.g. the BASE, SYN-ENSO and DRY3 scenarios – facilitate stable coexistence and promote diversity (Figs 7a,d, 9b, S5). Coexistence occurs because the hydroclimates of each scenario produce a mortality dynamic that opens favorable light and water niche spaces for each PFT to periodically outcompete the other three (Fig. 4c). The frequency of strong El Niño-related droughts over many tropical forests is predicted to increase over this century (Cai *et al*., 2014). At BCI, strong El Niño-related droughts often manifest as a 4- to 8-wk increase in the dry season length, followed by relatively heavy rains during the subsequent La Niña phase (Ropelewski & Halpert, 1987). Accordingly, the DRY3 scenario is most analogous to an increase in the frequency of strong El Niño-related droughts. ED2-hydro predicts that such an increase in El Niño-related droughts will have a minimal impact on the functional diversity and AGB of moist evergreen tropical forests (Fig. S5).

The stability in predicted total AGB (Fig. 3) arises from fast recoveries (i.e. *c*. 2–3 yr) following disturbances through both heavy recruitment pulses and elevated growth leading to infilling of the surviving trees, as is typical in moist evergreen tropical forests (Zimmerman *et al*., 2014, Condit *et al*., 2017a; Meakem *et al*., 2017). Similarly at BCI, the 33-yr observation

period (1982–2015) contained two major El Niños, 1982–1983 and 1997–1998, and total AGB remained relatively stable (Condit *et al*., 2012a). Yet, at the species level at BCI there were differential demographic responses to the 1982 drought where many moisture-demanding species experienced prolonged (10–15 yr) reductions in abundances and then subsequent recoveries (Condit *et al*., 2017a). While AGB may remain relatively stable over time in moist tropical forests, disturbance-related recruitment-pulses and infilling can set the trajectory of species composition for many decades (Lugo *et al*., 2000), which is consistent with the ED2-hydro prediction that PFT-specific fluctuations are not tightly coupled to inter-annual fluctuations in precipitation.

If the hydroclimate shifts towards being chronically drier—e.g., the DRY1, DRY2, DRY-WS, and DRY-DS— ED2-hydro predicts a reduction in functional diversity (Fig. 9b) characterized by a significant and compensatory shift toward drought-tolerant species (Fig. 7e–h), which is linearly proportional to the reduction in PAW (Fig. 9a). Interestingly, if the shift is toward a chronically drier dry season, ED2-hydro predicts that the compensatory infilling of drought-tolerant species will be moderated (Figs 7i, 8). On the other hand, if droughts become very rare or the hydroclimate becomes wetter (e.g. AVG or WET scenarios), as may be the case for regions of Southeast Asia (IPPC, 2014), ED2-hydro predicts a reduction in functional diversity (Fig. 9b) that arises from an increase in drought-intolerant PFTs (Fig. 9a).

This version of ED2-hydro defines hydraulic functional diversity through two contrasting levels of drought-tolerance. However, trees use numerous strategies to compete for light and water resources not explicitly represented in the model, which may produce different dynamics in other tropical forests. For example, drought-avoidance through hydraulic trait plasticity (Campanello *et al*., 2008), root niche separation (Ivanov *et al*., 2012), and drought-deciduousness (Xu *et al*., 2016) are prevalent in tropical systems that experience routine water-stress. Also, the effects of severe drought may be underestimated in this study because all drought-related mortality arises through C-starvation and not through hydraulic failure. Therefore, incorporating mortality that derives independently from hydraulic failure and drought-avoidance are important next-steps for fully predicting the effects of drought on tropical forests.

Conclusions

The strong agreement between model predictions and observed benchmarks in this study supports using size-structured forest models with hydrodynamics to make assessments about the consequences of drought on tropical forests. Our results show that the representation of functional diversity along only two trait axes allows total AGB of moist tropical forests to be resilient to variations in the precipitation regime despite changes in the functional composition of the forest. Accordingly, periodic severe droughts, such as those related to El Niño events, can have a stabilizing effect on coexistence and functional diversity, but highly-frequent or infrequent droughts may destabilize the community. Our results also identify climatic thresholds beyond which functional diversity is unable to maintain biomass stability. Thus, severe reductions in the amount of soil water available to plants during dry seasons may increase the vulnerability of moist tropical forests to significant reductions in AGB.

Acknowledgements

This research was supported as part of the Next Generation Ecosystem Experiments-Tropics, funded by the US Department of Energy, Office of Science, Office of Biological and Environmental Research. The raw data was provided by the Physical Monitoring Program of the Smithsonian Tropical Research Institute. We are grateful to Steve Paton and Ben Turner for providing the BCI meteorological and soil data.

Author contributions

T.L.P., L.M.K., C.D.K., R.A.F., N.G.M. and J.Q.C. planned and designed the research. T.L.P performed model experiments and analysis. T.L.P., B.F., D.J.J., R.G.K. analyzed observations. S.J.W. guided interpretation of BCI observations. R.C. and S.P.H. furnished the publicly archived BCI data. T.L.P., L.M.K., C.D.K., B.F., R.A.F., D.J.J., R.G.K., N.G.M., S.J.W. and J.Q.C. wrote the manuscript.

ORCID

Thomas L. Powell http://orcid.org/0000-0002-3516-7164

Daniel J. Johnson http://orcid.org/0000-0002-8585-2143

References

Bohrer G, Mourad H, Laursen TA, Drewry D, Avissar R, Poggi D, Oren R, Katul GG. 2005. Finite element tree crown hydrodynamics model (FETCH) using porous media flow within branching elements: A new representation of tree hydrodynamics. *Water Resources Research* **41**. doi:10.1029/2005WR004181.

Boisier JP, Ciais P, Ducharne A, Guimberteau M. 2015. Projected strengthening of Amazonian dry season by constrained climate model simulations. *Nature Climate Change* **5:** 656-660.

Bonan GB. 2008. Forests and climate change: forcings, feedbacks, and the climate benefits of forests. *Science* **320:** 1444.

Brodribb TJ, Holbrook NM, Edwards EJ, Gutiérrez MV. 2003. Relations between stomatal closure, leaf turgor and xylem vulnerability in eight tropical dry forest trees. *Plant, Cell & Environment* **26:** 433-450.

Cai W, Borlace S, Lengaigne M, van Rensch P, Collins M, Vecchi G, Timmermann A, Santoso A, McPhaden MJ, Wu L, England MH, Wang G, Guilyardi E, Jin F-F. 2014. Increasing frequency of extreme El Niño events due to greenhouse warming. *Nature Climate Change* **4:** 111-116.

Campanello PI, Gatti MG, Goldstein G. 2008. Coordination between water-transport efficiency and photosynthetic capacity in canopy tree species at different growth irradiances. *Tree Physiology* **28:** 85-94.

Carrasco LO, Bucci SJ, Di Francescantonio D, Lezcano OA, Campanello PI, Scholz FG, Rodríguez S, Madanes N, Cristiano PM, Hao G-Y, Holbrook NM, Goldstein G. 2015. Water storage dynamics in the main stem of subtropical tree species differing in wood density, growth rate and life history traits. *Tree Physiology* **35:** 354-365.

Castanho ADA, Coe MT, Costa MH, Malhi Y, Galbraith D, Quesada CA. 2013. Improving simulated Amazon forest biomass and productivity by including spatial variation in biophysical parameters. *Biogeosciences* **10:** 2255-2272.

Chave J, Condit R, Lao S, Caspersen JP, Foster RB, Hubbell SP. 2003. Spatial and temporal variation of biomass in a tropical forest: results from a large census plot in Panama. *Journal of Ecology* **91:** 240-252.

Chesson P. 2000. Mechanisms of maintenance of species diversity. *Annual Review of Ecology and Systematics* **31:** 343-366.

Christoffersen BO, Gloor M, Fauset S, Fyllas NM, Galbraith DR, Baker TR, Kruijt B, Rowland L, Fisher, Binks OJ *et al*. 2016. Linking hydraulic traits to tropical forest function in a size-structured and trait-driven model (TFS v.1-Hydro). *Geoscientific Model Development* **9**. doi: 10.5194/gmd-9-1-2016.

Clapp RB, Hornberger GM. 1978. Empirical equation for some soil hydraulic properties. *Water Resources Research* **14:** 601-604.

Clark DA, Asao S, Fisher R, Reed S, Reich PB, Ryan MG, Wood TE, Yang X. 2017. Reviews and syntheses: Field data to benchmark the carbon-cycle models for tropical forests. *Biogeosciences* **14:** 4663-4690.

Condit R. 1998. *Tropical forest census plots: methods and results from Barro Colorado Island, Panama and a comparison with other plots.* Berlin, Germany: Springer-Verlag.

Condit R, Hubbell SP, Foster RB. 1995. Mortality rates of 205 neotropical tree and shrub species and the impact of a severe drought. *Ecological Monographs* **65:** 419-439.

Condit R, Watts K, Bohlman SA, Pérez R, Foster RB, Hubbell SP. 2000. Quantifying the deciduousness of tropical canopies under varying climates. *Journal of Vegetation Science* **11:** 649-658.

Condit R, Lao S, Pérez R, Dolins SB, Foster RB, Hubbell SP. 2012a. Barro Colorado Forest Census Plot Data, 2012 Version. Center for Tropical Forest Science Databases. DOI http://dx.doi.org/10.5479/data.bci.20130603. [accessed 11 March 2016].

Condit R, Chisholm RA, Hubbell SP. 2012b. Thirty years of forest census at Barro Colorado and the importance of immigration in maintaining diversity. *PLoS ONE* **7:** e49826.

Condit R, Engelbrecht BMJ, Pino D, Pérez R, Turner BL. 2013. Species distributions in response to individual soil nutrients and seasonal drought across a community of tropical trees. *Proceedings of the National Academy of Sciences* **110:** 5064-5068.

Condit R, Pérez R, Lao S, Aguilar S, Hubbell SP. 2017a. Demographic trends and climate over 35 years in the Barro Colorado 50 ha plot. *Forest Ecosystems* **4**. doi: 10.1186/s40663-017-0103-1

Condit R, Aguilar S, Pérez R, Lao S, Hubbell SP, Foster RB. 2017b. BCI 50-ha Plot Taxonomy as of 2017. DOI https://doi.org/10.25570/stri/10088/32990. [accessed 15 May 2018].

da Costa ACL, Galbraith D, Almeida S, Portela BTT, da Costa M, de Athaydes Silva Junior J, Braga AP, de Gonçalves PHL, de Oliveira AAR, Fisher R, Phillips OL *et al.* 2010. Effect of 7 yr of experimental drought on vegetation dynamics and biomass storage of an eastern Amazonian rainforest. *New Phytologist* **187:** 579–591.

Dirzo R, Raven PH. 2003. Global state of biodiversity and loss. *Annual Review of Environment and Resources* **28**: 137-167.

Fauset S, Baker TR, Lewis SL, Feldpausch TR, Affum-Baffoe K, Foli EG, Hamer KC, Swaine MD. 2012. Drought-induced shifts in the floristic and functional composition of tropical forests in Ghana. *Ecology Letters* **15**: 1120-1129.

Fisher RA, Koven CD, Anderegg WRL, Christoffersen BO, Dietze MC, Farrior C, Holm JA, Hurtt G, Knox RG, Lawrence PJ, et al. 2018. Vegetation demographics in Earth System Models: a review of progress and priorities. *Global Change Biology* **24:** 35-54.

Galbraith D, Malhi Y, Affum-Baffoe K, Castanho ADA, Doughty CE, Fisher RA, Lewis SL, Peh KSH, Phillips OL, Quesada CA, et al. 2013. Residence times of woody biomass in tropical forests. *Plant Ecology and Diversity* **6:** 139-157.

Goudriaan J. 1977. *Crop micrometeorology: a simulation study.* Wageningen, the Netherlands: Center for Agricultural Publishing and Documentation.

IPCC. 2014. Pachauri RK, Meyer LA, eds. *Climate Change 2014: Synthesis Report*. *Contribution of Working Groups I, II and III to the Fifth Assessment Report of the Intergovernmental Panel on Climate Change*. IPCC, Geneva, Switzerland.

Ivanov VY, Hutyra LR, Wofsy SC, Munger JW, Saleska SR, de Oliveira Jr. RC, de Camargo PB. 2012. Root niche separation can explain avoidance of seasonal drought stress and vulnerability of overstory trees to extended drought in a mature Amazonian forest. *Water Resoures Research* **48:** W12507.

Joetzjer E, Douville H, Delire C, Ciais P. 2013. Present-day and future Amazonian precipitation in global climate models: CMIP5 versus CMIP3. *Climate Dynamics* **41:** 2921-2936.

King DA, Davies SJ, Tan S, Nur Supardi MN. 2006. The role of wood density and stem support costs in the growth and mortality of tropical trees: tree demography and stem support costs. *Journal of Ecology* **94:** 670–80.

Knox RG, Longo M, Swann ALS, Zhang K, Levine NM, Moorcroft PR, Bras RL. 2015. Hydrometeorological effects of historical land-conversion in an ecosystem-atmosphere model of northern South America. *Hydrology and Earth System Sciences* **19:** 241-273.

Levine NM, Zhang K, Longo M, Baccini A, Phillips OL, Lewis SL, Alvarez-Dávila E, de Andrade ACS, Brienen RJ, Erwin TL, Feldpausch TR. 2016. Ecosystem heterogeneity determines the ecological resilience of the Amazon to climate change. *Proceedings of the National Academy of Sciences* **113:** 793-797.

Li W, Fu R, Dickinson RE. 2006. Rainfall and its seasonality over the Amazon in the 21st century as assessed by the coupled models for the IPCC AR4. *Journal of Geophysical Research* **111:** D02111.

Lima LS, Coe MT, Soares Filho BS, Cuadra SV, Dias LCP, Costa MH, Lima LS, Rodrigues HO. 2014. Feedbacks between deforestation, climate, and hydrology in the Southwestern Amazon: implications for the provision of ecosystem services. *Landscape Ecology* **29:** 261-274.

Lugo A, Figueroa Colón J, Scatena F. 2000. The Caribbean. In: Barbour MG, Billings, WD, eds. *North American terrestrial vegetation, second edition*. Cambridge, UK: Cambridge University Press, 594–622.

Meakem V, Tepley AJ, Gonzalez-Akre EB, Herrmann V, Muller-Landau HC, Wright SJ, Hubbell SP, Condit R, Anderson-Teixeira KJ. 2017. Role of tree size in moist tropical forest carbon cycling and water deficit responses. *New Phytologist*. doi: 10.1111/nph.14633.

Medvigy D, Wofsy SC, Munger JW, Hollinger DY, Moorcroft PR. 2009. Mechanistic scaling of ecosystem function and dynamics in space and time: Ecosystem Demography model version 2. *Journal of Geophysical Research* **114:** G01002.

Meinzer FC, James SA, Goldstein G, Woodruff D. 2003. Whole-tree water transport scales with sapwood capacitance in tropical forest campy trees. *Plant, Cell & Environment* **26:** 1147-1155.

Meir P, Wood TE, Galbraith DR, Brando PM, da Costa ACL, Rowland L, Ferreira LV. 2015. Threshold responses to soil moisture deficit by trees and soil in tropical rain forests: insights from field experiments. *BioScience* **65:** 882-892.

Miller SD, Goulden ML, Hutyra LR, Keller M, Saleska SR, Wofsy SC, Figueira AMS, da Rocha HR, de Camargo PB. 2011. Reduced impact logging minimally alters tropical rainforest carbon and energy exchange. *Proceedings of the National Academy of Sciences* **108:** 19431-19435.

Moorcroft PR, Hurtt GC, Pacala SW. 2001. A method for scaling vegetation dynamics: the Ecosystem Demography model (ED). *Ecological Monographs* **71:** 557-587.

Muller-Landau HC. 2004. Interspecific and inter-site variation in wood specific gravity of tropical trees. *Biotropica* **36:** 20–32.

Nepstad DC, Tohver IM, Ray D, Moutinho P, Cardinot G. 2007. Mortality of large trees and lianas following experimental drought in an Amazon forest. *Ecology* **88:** 2259-2269.

Pan Y, Birdsey RA, Fang J, Houghton RA, Kauppi PE, Kurz WA, Phillips OL, Shvidenko A, Lewis SL, Canadell JG, et al. 2011. A Large and persistent carbon sink in the world's forests. *Science* **333:** 988-993.

Poorter L, McDonald I, Alarcon A, Fichtler E, Licona J-C, Peña-Claros M, Sterck F, Villegas Z, Sass-Klaassen U. 2010. The importance of wood traits and hydraulic conductance for the performance and life history strategies of 42 rainforest tree species. *New Phytologist* **185:** 481-492.

Powell T, Faybishenko B, Kueppers L, Paton S. 2018. Seven years (2008-2014) of meteorological observations plus a synthetic El Niño drought for BCI Panama. NGEE Tropics Data Collection. Accessed at http://dx.doi.org/10.15486/ngt/1414275

Powell TL. 2015. *Determining drought sensitivity of the Amazon forest: does plant hydraulics matter?* PhD thesis, Harvard University, Cambridge, MA, USA. http://nrs.harvard.edu/urn-3:HUL.InstRepos:23845447

Powell TL, Galbraith DR, Christoffersen BO, Harper A, Imbuzeiro HMA, Rowland L, Almeida A, Brando PM, da Costa ACL, Costa MH *et al*. 2013. Confronting model predictions of carbon fluxes with measurements of Amazon forests subjected to experimental drought. *New Phytologist* **200:** 350-364.

Powell TL, Wheeler JK, de Oliveira AAR, da Costa ACL, Saleska SR, Meir P, Moorcroft PR. 2017. Differences in xylem cavitation resistance and leaf hydraulic traits explain differences in drought tolerance among mature Amazon rainforest trees. *Global Change Biology* **23:** 4280-4293.

Reich PB. 2014. The world-wide 'fast–slow' plant economics spectrum: a traits manifesto. *Journal of Ecology* **102:** 275-301.

Ropelewski CF, Halpert MS. 1987. Global and regional scale precipitation patterns associated with the El Niño/Southern Oscillation. *Monthly Weather Review* **115:** 1606-1626.

Rowland L, da Costa ACL, Galbraith DR, Oliveira RS, Binks OJ, Oliveira AAR, Pullen AM, Doughty CE, Metcalfe DB, Vasconcelos SS *et al*. 2015. Death from drought in tropical forests is triggered by hydraulics not carbon starvation. *Nature* **528:** 119-122.

Sakschewski B, von Bloh W, Boit A, Poorter L, Peña-Claros M, Heinke J, Joshi J, Thonicke K. 2016. Resilience of Amazon forests emerges from plant trait diversity. *Nature Climate Change* **6:** 1032-1036.

Sterck F, Markesteijn L, Schieving F, Poorter L. 2011. Functional traits determine trade-offs and niches in a tropical forest community. *Proceedings of the National Academy of Sciences* ***108*****:** 20627-20632.

Sumila TCA, Pires GF, Fontes VC, Costa MH. 2017. Sources of water vapor to economically relevant regions in Amazonia and the effects of deforestation. *Journal of Hydrometeorology* **18:** 1643-1655.

Weng ES, Malyshev S, Lichstein JW, Farrior CE, Dybzinski R, Zhang T, Shevliakova E, Pacala SW. 2015. Scaling from individual trees to forests in an Earth system modeling framework using a mathematically tractable model of height-structured competition. *Biogeosciences* **12:** 2655-2694.

Williams M, Rastetter EB, Fernandes DN, Goulden ML, Wofsy SC, Shaver GR, Melillo JM, Munger JW, Fan S-M, Nadelhoffer KJ. 1996. Modelling the soil-plant-atmosphere continuum in a *Quercus–Acer* stand at Harvard Forest: the regulation of stomatal conductance by light, nitrogen and soil/plant hydraulic properties. *Plant, Cell & Environment* **19:** 911–927.

Williams M, Law BE, Anthoni PM, Unsworth MH. 2001. Use of a simulation model and ecosystem flux data to examine carbon–water interactions in ponderosa pine. *Tree Physiology* **21:** 287-298.

Wright SJ. 2002. Plant diversity in tropical forests: a review of mechanisms of species coexistence. *Oecologia* **130:** 1-14.

Wright SJ, Kitajima K, Kraft NJB, Reich PB, Wright IJ, Bunker DE, Condit R, Dalling JW, Davies SJ, Díaz S, *et al.* 2010. Functional traits and the growth-mortality trade-off in tropical trees. *Ecology* **91:** 3664-3674.

Xu X, Medvigy D, Powers J, Becknell J, Guan K. 2016. Hydrological niche separation explains seasonal and inter-annual variations in seasonally dry tropical forests. *New Phytologist* **212:** 80-95.

Young DJN, Stevens JT, Earles JM, Moore J, Ellis A, Jirka AL, Latimer AM. 2017. Long-term climate and competition explain forest mortality patterns under extreme climate. *Ecology Letters* **20:** 78-86.

Zhang K, Castanho ADDA, Galbraith DR, Moghim S, Levine NM, Bras RL, Coe MT, Costa MH, Malhi Y, Longo M. et al. 2015. The fate of the Amazonian ecosystems over the coming century arising from changes in climate, atmospheric CO_2, and land use. *Global Change Biology* **21:** 2569–2587.

Zimmerman JK, Hogan JA, Shiels AB, Bithorn JE, Carmona SM, Brokaw N. 2014. Seven-year responses of trees to experimental hurricane effects in a tropical rainforest, Puerto Rico. *Forest Ecology and Management* **332:** 64-74

Supporting Information

Additional Supporting Information may be found online in the Supporting Information tab for this article:

Fig. S1 Basal area and mortality size-class distributions of all observed species and canopy-only species compared to model predictions.

Fig. S2 Example of how the meteorology of August 2013 was modified to reflect August 1982.

Fig. S3 Example of how the meteorology of April 2008 was modified to reflect April 1983.

Fig. S4 Initial 4 yr of the bare ground spin up of aboveground biomass at Barro Colorado Island, Panama.

Fig. S5 Simulated aboveground biomass dynamics for Barro Colorado Island, Panama, under the DRY3 precipitation scenario.

Fig. S6 Simulated total aboveground biomass for each precipitation scenario plotted against the mean annual plant available soil water.

Fig. S7 Simulated aboveground biomass dynamics of Barro Colorado Island, Panama, with a prescribed 5 m rooting depth.

Fig. S8 Simulated aboveground biomass dynamics for Barro Colorado Island, Panama, under each of the precipitation scenarios with a prescribed 5 m rooting depth.

Fig. S9 Total aboveground biomass for each precipitation scenario plotted against the plant available soil water using a prescribed 5 m rooting depth.

Fig. S10 Ecosystem diversity under each precipitation scenario plotted against mean plant available soil water using a prescribed 5 m rooting depth.

Table S1 Months selected to create the synthetic 1982 – 1983 El Nino period at BCI, Panama

Notes S1 Description of meteorological drivers for precipitation scenarios.

Notes S2 Description of El Niño meteorological drivers.

Notes S3 Barro Colorado Island Meteorological Drivers for 2008 to 2010.

Notes S4 ED2_hydro source code and parameter files.

Notes S5 Description of model sensitivity to an increase in plant available soil water.

Fig. 1 Long-term (1930–2014) annual precipitation recorded at a nearby weather station (LT-obs, gray) compared to a 7-yr record of locally observed precipitation at Barro Colorado Island, Panama. The local precipitation was used for the spin-up and baseline simulations (BASE, red). Solid horizontal line indicates the long-term mean (2662 mm) of LT-obs. Dashed lines indicate ± 1 SD (479 mm).

Fig. 2 Mean monthly precipitation from the baseline meteorological drivers (BASE, red) compared to (a) long-term (1930–2014) observed mean monthly precipitation (LT-Obs, grey)

and (b) monthly precipitation for the years representing average precipitation (AVG, magenta stars) and the 3-month extended dry-season (DRY1, blue triangles). (c) Observed long-term (1930–2014) monthly precipitation (LT-Obs, solid grey circles) compared monthly precipitation from the observations during the 1982-1983 El Niño (obs-enso, open black circles) and the synthetic El Niño meteorological drivers (syn-enso, open red triangle). In all panels, the symbols mark the means and the grey and dashed-red polygons mark ±1 SD.

Fig. 3 Simulated aboveground biomass (AGB, kg C m^{-2}) dynamics of Barro Colorado Island (BCI), Panama, for 1000 yr from a bare ground spin-up using the baseline (BASE) meteorology. Simulated total AGB (black curve) is compared to a measured estimation of 14.0 ± 1.0 kg C m^{-2} (red symbol) for the 50-ha plot (Chave *et al*., 2003). AGB of the four tropical tree plant functional types are early-successional drought-tolerant (early-dt, dark blue), early-successional drought-intolerant (early-di, light blue), late-successional drought-tolerant (late-dt, dark red), late-successional drought-intolerant (late-di, light red). The arrow indicates the initialization point for the drought scenario simulations.

Fig. 4 Mortality rates (yr^{-1}) of trees > 10 cm dbh on Barro Colorado Island (BCI), Panama, over 30 yr. (a) Simulated (black solid line) versus the observed range (grey dashed line) of total ecosystem mortality rates from the six 5-yr census intervals between 1982–2010 (Condit *et al*. 2012a). El Niño, dry and wet years are noted for the meteorological forcing of the model with arrows. (b) Mortality rates of the four plant functional types are early-successional drought-tolerant (early-dt, dark blue), early-successional drought-intolerant (early-di, light blue), late-successional drought-tolerant (late-dt, dark red), late-successional drought-intolerant (late-di, light red). (c) Simulated differences (Δ) in mortality rates (yr^{-1}) for drought-tolerant versus drought-intolerant (e.g Δ = drought-tolerant – drought-intolerant) within the early-successional (blue) and late-successional (red) plant functional types. Horizontal line indicates 0 difference, above the zero line favors drought-intolerant, below favors drought-tolerant.

Fig. 5 Size-class distributions of observed (open circles) and modeled (grey bars) basal area (m^{-2} ha^{-1}) and mortality rates (yr^{-1}) in the 50-ha plot at Barro Colorado Island, Panama. Basal areas per size-class for (a) early- and (b) late-successional trees and (c) for the total ecosystem.

Mortality rates per size-class for (d) early- and (e) late-successional trees and (f) the total ecosystem. Observed basal area and mortality rates are from the 2005 and 2005–2010 censuses, respectively, (Condit *et al*., 2012a). Model predictions are at the end of the 1000 yr spin-up. Size-class bins are noted by their lower boundaries.

Fig. 6 Modeled (open square) and observed (closed circle) relationship between the wood density (g cm^{-3}) and mortality rates (% yr^{-1}) of canopy tree species. Each observed data point represents canopy tree species binned into quartiles that operate along the light demanding to shade tolerance continuum reported in Wright *et al*. (2010). Observations are reported as mean ± SD.

Fig. 7 Simulated aboveground biomass (kg C m^{-2}) dynamics for Barro Colorado Island (BCI), Panama, under each of the precipitation scenarios. The four plant functional types are shown are early-successional drought-tolerant (early-dt, dark blue), early-successional drought-intolerant (early-di, light blue), late-successional drought-tolerant (late-dt, dark red), late-successional drought-intolerant (late-di, light red). (a) BASE, baseline precipitation scenario. (b) AVG, monthly average precipitation. (c) WET, 30% increase in precipitation. (d) SYN-ENSO, includes a severe El Niño drought every 20 yr. (e) DRY-WS, 40% reduction in wet season precipitation. (f) DRY-DS, 75% reduction in dry season precipitation. (g, h) Three-month lengthening of the dry season every year (DRY1) and every other year (DRY2). (i) Total aboveground biomass across all precipitation scenarios (grey lines) with DRY-DS emphasized (black line) compared to observations (red symbol, mean ± 95% CI, Chave *et al*., 2003). All simulations were initialized from year 700 of the 1000 yr spin-up of BASE.

Fig. 8 Total aboveground biomass (AGB, kg C m^{-2}) at the end of the 400-yr simulation for each of the precipitation scenarios plotted against the long-term mean of plant available soil water (PAW, mm) in the rooting zone (3 m depth) during the late dry-season (i.e. PAW of March and April). Precipitation scenarios: BASE, baseline precipitation; AVG, long-term average precipitation of each month; ENSO, includes a severe El Niño drought every 20 yr; DRY1, 3 month increase in the dry season each year; DRY2, 3 month increase in the dry season every 2nd year; DRY3, 3 month increase in the dry season every 3rd year; DRY-WS, 40% decrease in the

wet season precipitation; DRY-DS, 75% decrease in the dry season precipitation; WET, 30% increase in precipitation. Red symbol denotes DRY-DS, which is significantly lower than the observed AGB. All black symbols are within the error of observed AGB.

Fig. 9 Ecosystem diversity at the end of the 400-yr simulation for each precipitation scenario plotted against the mean plant available soil water (PAW, mm) for the last 10 yr of the simulation. (a) Ratio between drought-tolerant plant functional types (PFTs) and total ecosystem aboveground biomass: 0, drought-tolerant PFTs dominate; 1, drought-intolerant PFTs dominate. (b) Shannon-Wiener evenness index for the four simulated PFTs: 1, all four PFTs are completely even; 0, ecosystem is completely uneven and one PFT dominates. Precipitation scenarios: BASE, baseline precipitation; AVG, long-term average precipitation of each month; ENSO, includes a severe El Niño drought every 20 yr; DRY1, 3 month increase in the dry season each year; DRY2, 3 month increase in the dry season every 2nd year; DRY3, 3 month increase in the dry season every 3rd year; DRY-WS, 40% decrease in the wet season precipitation; DRY-DS, 75% decrease in the dry season precipitation; WET, 30% increase in precipitation.

Table 1 Explanation of plant functional type symbols, model parameters, and equations used in this study

Symbol	Definition	Value	Units	Source code name	Source
Plant functional type (PFT) definitions:					
early	Early-successional				
late	Late-successional				
dt	Drought-tolerant				
di	Drought-intolerant				
Model parameters:					
C_{leaf}	Leaf capacitance	3.0e-3	kg H_2O m^{-3} MPa^{-1}	*Cap_leaf*	This study
C_{stem}	Stem capacitance	204	kg H_2O m^{-3} MPa^{-1}	*Cap_stem*	Based on Meinzer *et al.* (2003); Carrasco *et al.* (2015)
H_{max}	Maximum tree height	38.0	m	*hgt_max*	This study
$K_{s,sat}$	Integrated root-to-shoot maximum conductivity when woody tissue is	early-dt: 1.6 early-di: 3.5	kg H_2O m^{-1} s^{-1} MPa^{-1}	*water_conductivity*	Tuned in this study. Initial values and relative differences

	saturated	late-dt: 0.7 late di: 1.4			based on Campanello *et al*. (2008)
TLP	Turgor loss point	dt: -2.5 di: -1.5	MPa	*TLP*	Powell *et al*. (2017)
VC	Vulnerability curve: scaling factor representing xylem vulnerability to cavitation.	range: 0–-1		*vuln_curve*	Powell (2015); Xu *et al*. (2016)
β	Scaling factor represent stomatal sensitivity to Ψ_{leaf}	range: 0–1		*fsw*	Powell (2015)
ρ_{wood}	Wood density	early: 0.40 late: 0.68	g cm^{-3}	*rho*	Based on Condit *et al.* (2012)
Ψ_{leaf}	Leaf water potential		MPa	*psi_leaf*	Xu *et al.* (2016)
Ψ_{xylem}	Xylem water potential		MPa	*psi_stem*	Xu *et al.* (2016)
$\Psi 50_{xylem}$	Xylem pressure at 50% loss of conductivity	dt: -2.2 di: -1.2	MPa	*psi50*	Powell *et al*. (2017)

Weibull equations for xylem cavitation and stomatal closure :						Powell (2015)
	$VC = e^{-\left(\frac{\psi_{xylem}}{c1}\right)^{c2}}$				(Eqn 3)	
	$\beta = e^{-\left(\frac{\psi_{leaf}}{c3}\right)^{c4}}$				(Eqn 4)	
c1	Empirical xylem-vulnerability curve parameter	dt: -2.55 di: -1.47	MPa	*c1*		Powell *et al*. (2017)
c2	Empirical xylem-vulnerability curve parameter	dt: 2.45 di: 1.8		*c2*		Powell *et al*. (2017)
c3	Empirical stomatal-closure curve parameter	dt: -2.83 di: -1.67	MPa	*c3*		Powell *et al*. (2017)
c4	Empirical stomatal-closure curve parameter	dt: 3.0 di: 3.5		*c4*		Powell *et al*. (2017)
Rooting depth equation:	$maximum\ rooting\ depth = b1 * (tree\ height)^{b2}$				(Eqn 5)	Powell *et al*. (2013)
b1	Rooting depth parameter	-0.815	m	*b1Rd*		This study

b2	Rooting depth parameter	0.365	unitless	*b2Rd*	This study

Mortality equations:

$$mortality_{total} = mortality_{cb} + mortality_{bg}(PFT) \quad \text{(Eqn 6a)}$$

Moorcroft *et al.* (2001)

$$mortality_{cb} = \frac{m1}{\left[1+e^{m2\left(\frac{Prod_{actual}}{Prod_{full\_sun}}\right)}\right]} \quad \text{(Eqn 6b)}$$

$$mortality_{bg}(PFT) = m4 + \left[m3 * \left(1 - \frac{\rho(PFT)}{\rho(PFT_{late})}\right)\right] \quad \text{(Eqn 6c)}$$

$mortality_{total}$	Total cohort mortality rate	yr^{-1}	mort_rate
$mortality_{cb}$	Number-density dependent negative carbon balance mortality rate	yr^{-1}	mort_rate(2)
$mortality_{bg}(PFT)$	PFT dependent background mortality rate	yr^{-1}	mort_rate(1,3)
$Prod_{actual}$	Actual net productivity of a cohort constrained by its environment.	kg-C $cohort^{-1}$ yr^{-1}	cb_act
$Prod_{full\_sun}$	Net productivity of a cohort if it were in full	kg-C $cohort^{-1}$	cb_max

	sunlight, high humidity and well-watered.		yr^{-1}		
m1	Carbon balance fitting parameter	7.5		mort1	This study
m2	Carbon balance fitting parameter	14.0		mort2	This study
m3	PFT dependent fitting parameter	0.1	yr^{-1}	mort3	This study
m4	Treefall disturbance rate	0.014	yr^{-1}	treefall_disturbance_rate	Moorcorft *et al*. (2001)

Note: unless individual PFTs values are provided, single values apply to all PFTs.

Table 2 Explanation of precipitation scenarios used as model experiments to examine effects of hydroclimate variation on forest biomass and functional composition

Scenario code name	Description
BASE	Baseline meteorology. Recycled 2008–2014 local meteorology.
AVG	Single-year recycled with long-term average monthly precipitation.
DRY1	3 month lengthening of dry season every year relative to AVG.
DRY2	3 month lengthening of dry season every other year relative to AVG.
DRY3	3 month lengthening of dry season every 3rd year relative to AVG.
DRY-WS	Drier wet season (May–December). 40% reduction relative to BASE.
DRY-DS	Drier dry season (January–April). 75% reduction relative to BASE.
SYN-ENSO	Included a strong El Niño once every 20 yr.
WET	30% increase in total precipitation (all months) relative to BASE

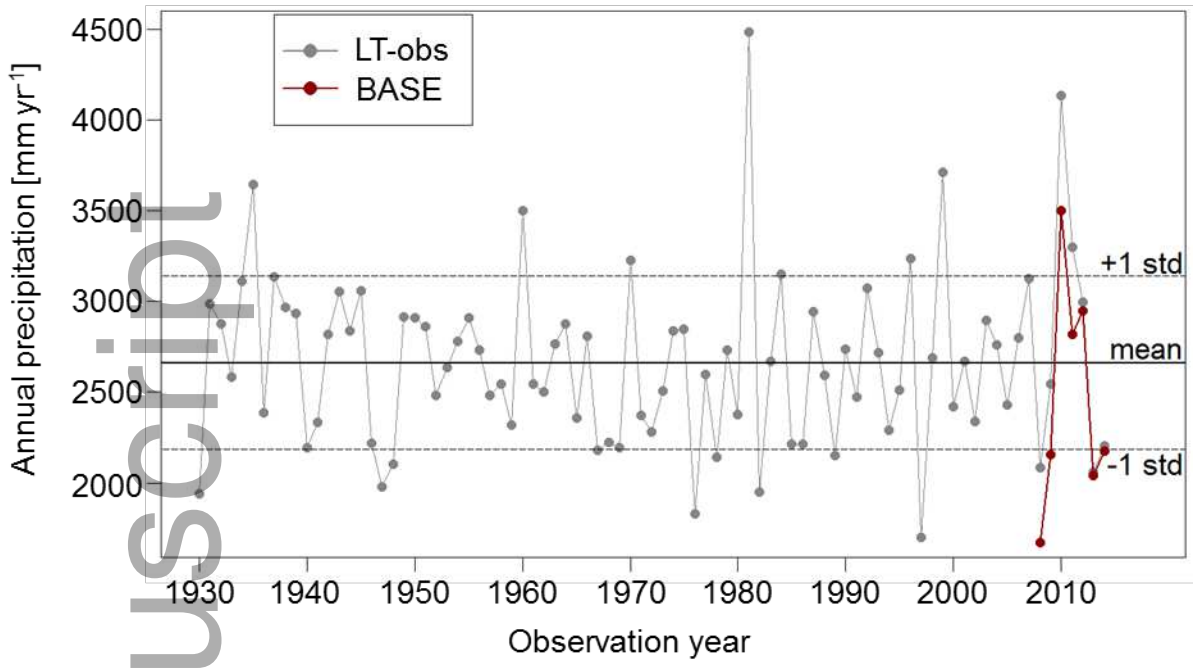

Fig. 1.

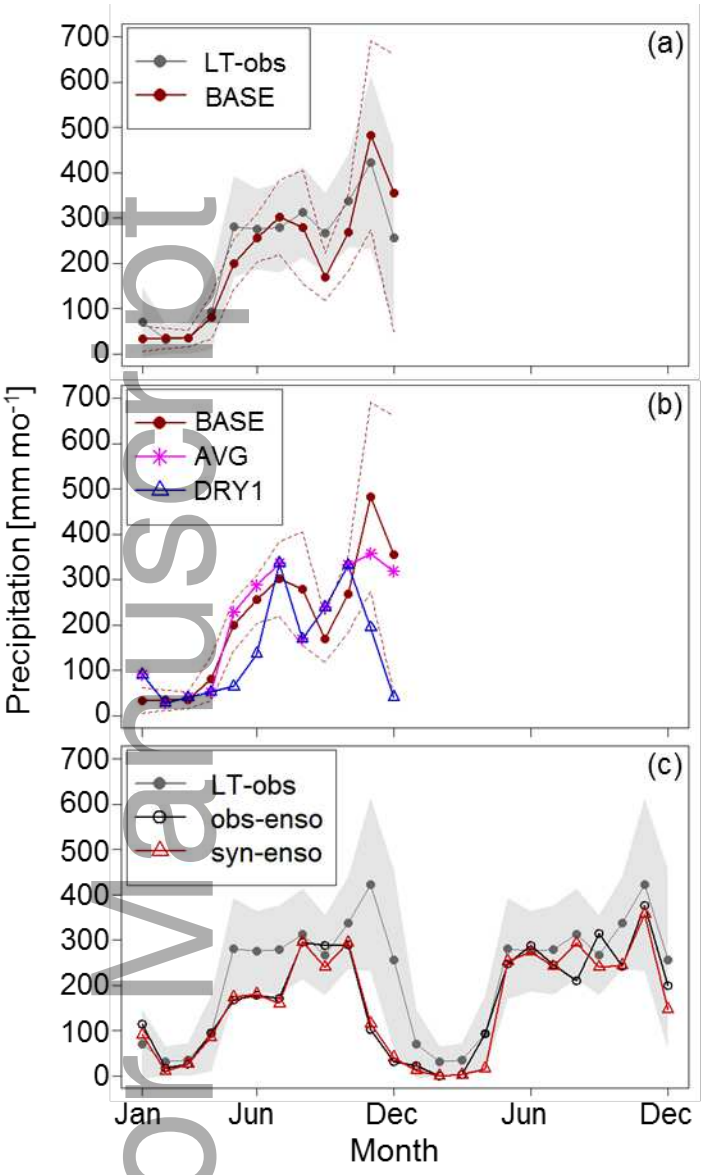

Fig. 2.

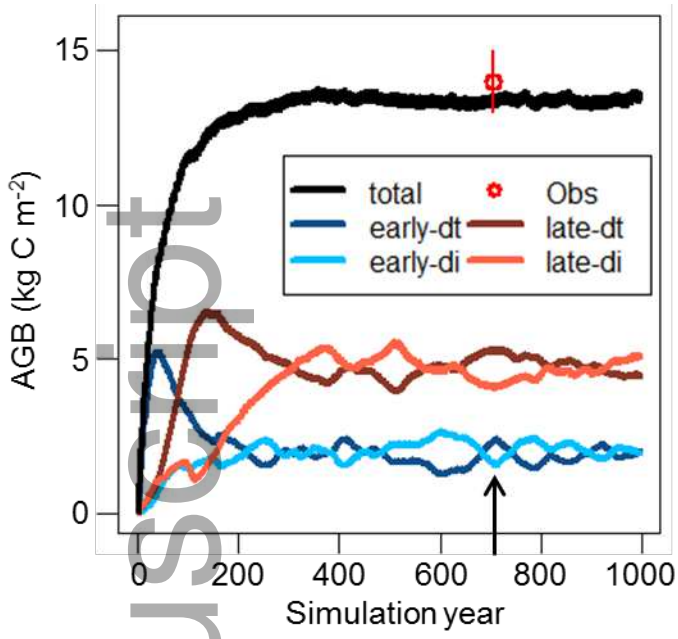

Fig. 3.

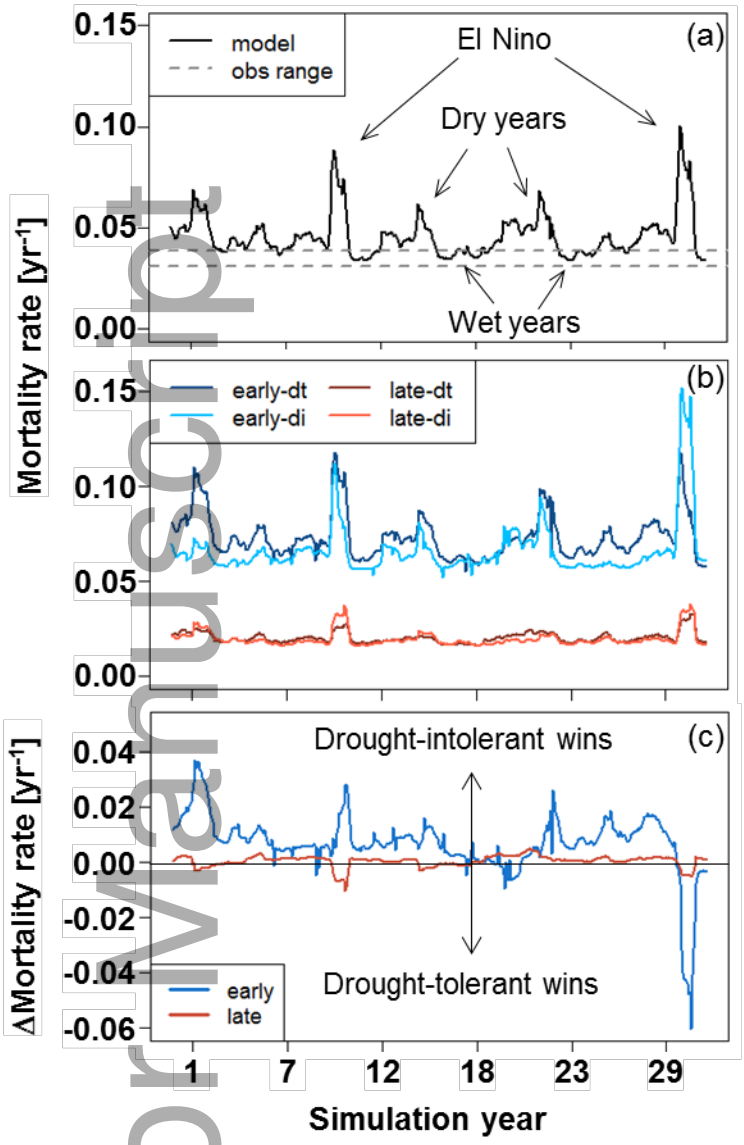

Fig. 4.

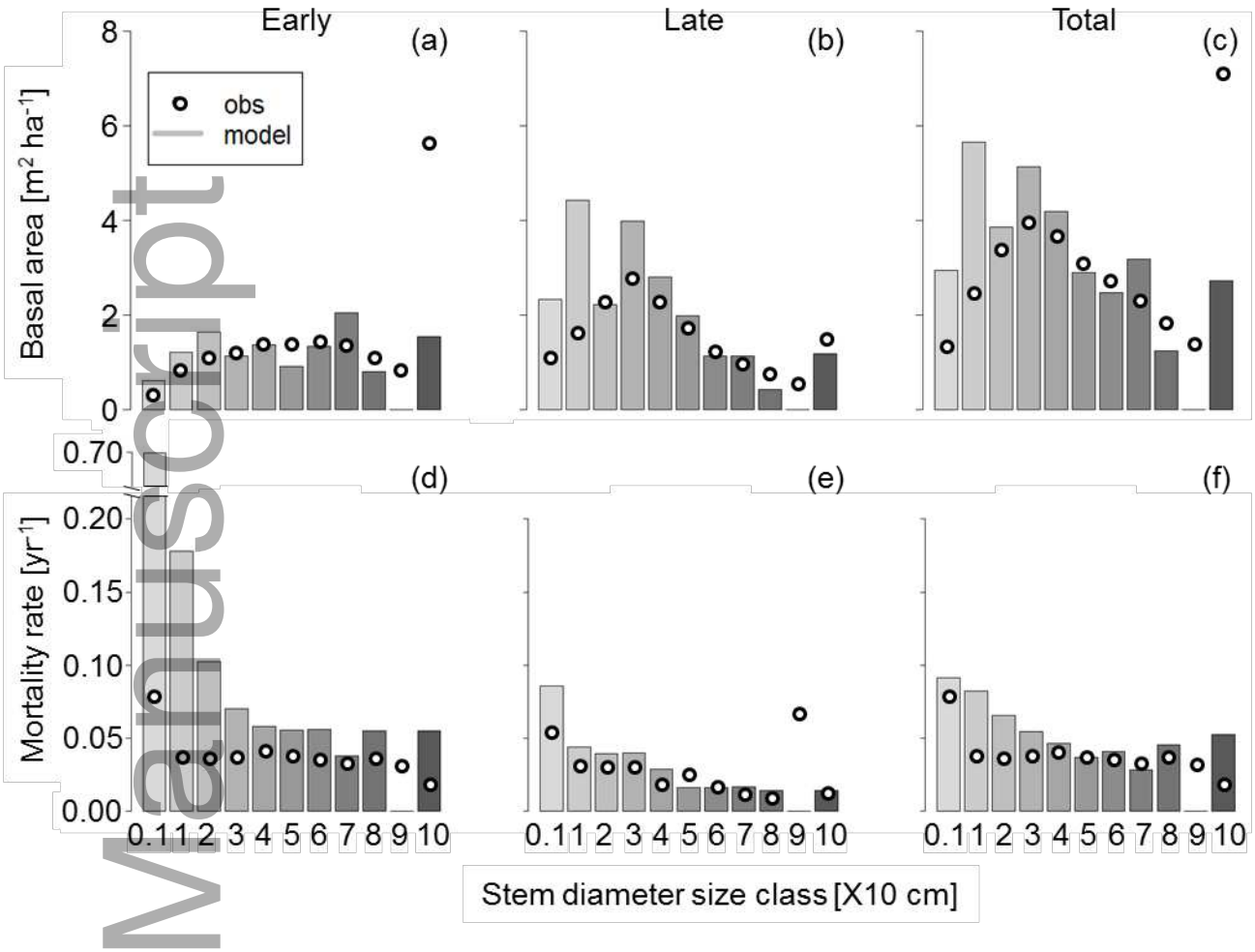

Fig. 5.

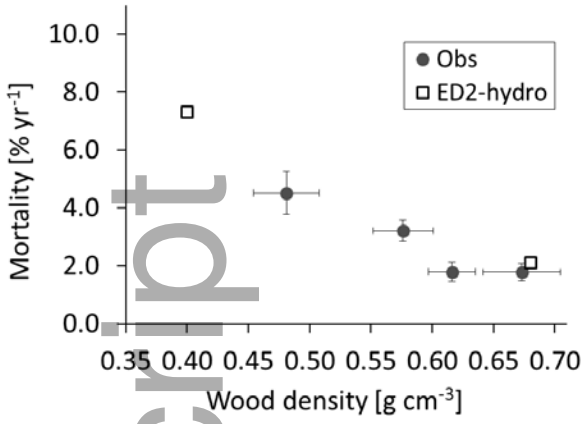

Fig. 6.

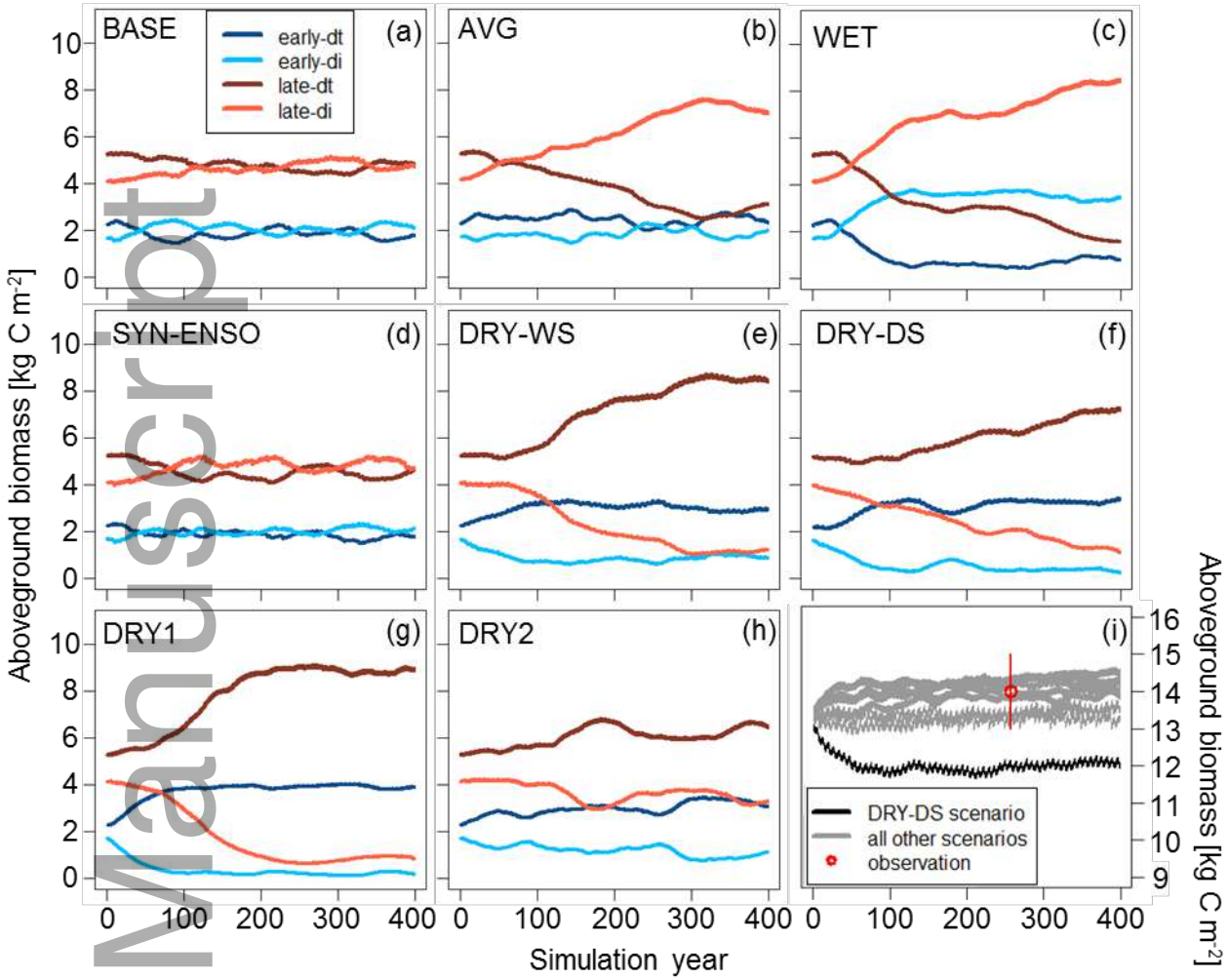

Fig. 7.

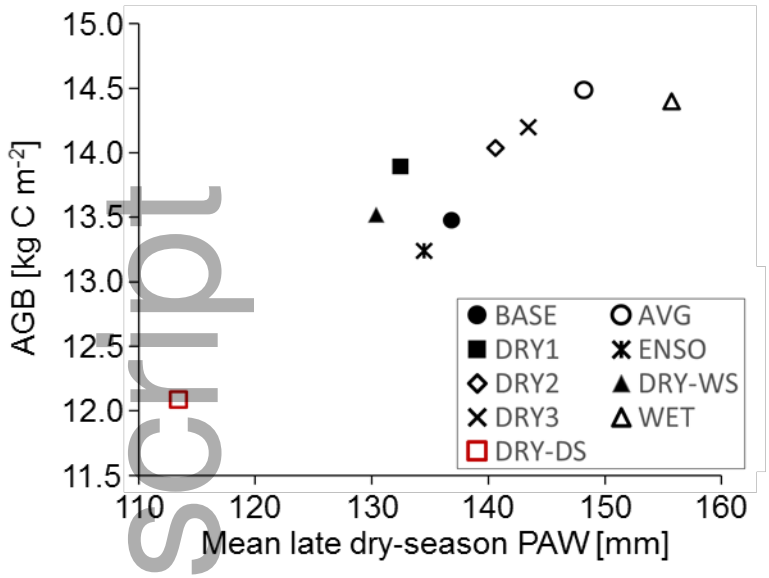

Fig. 8.

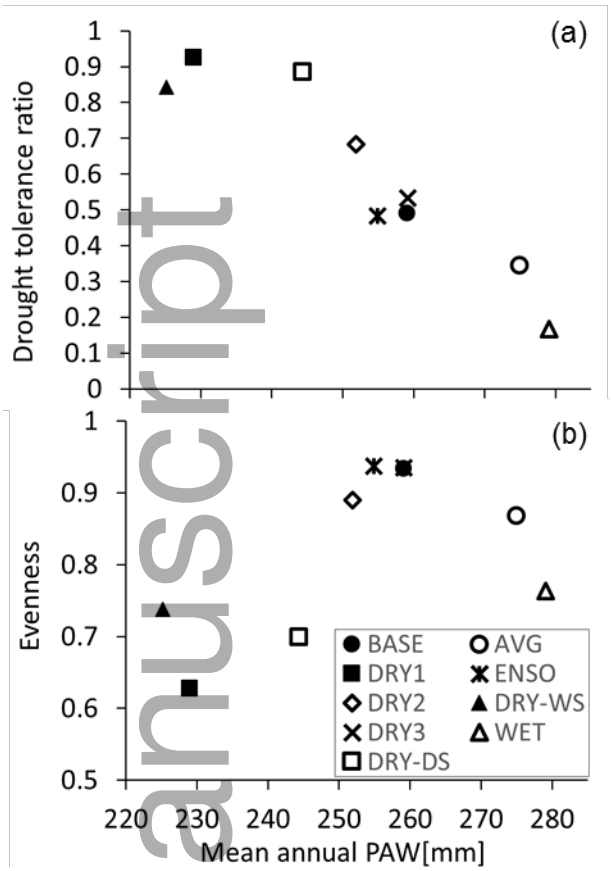

Fig. 9.

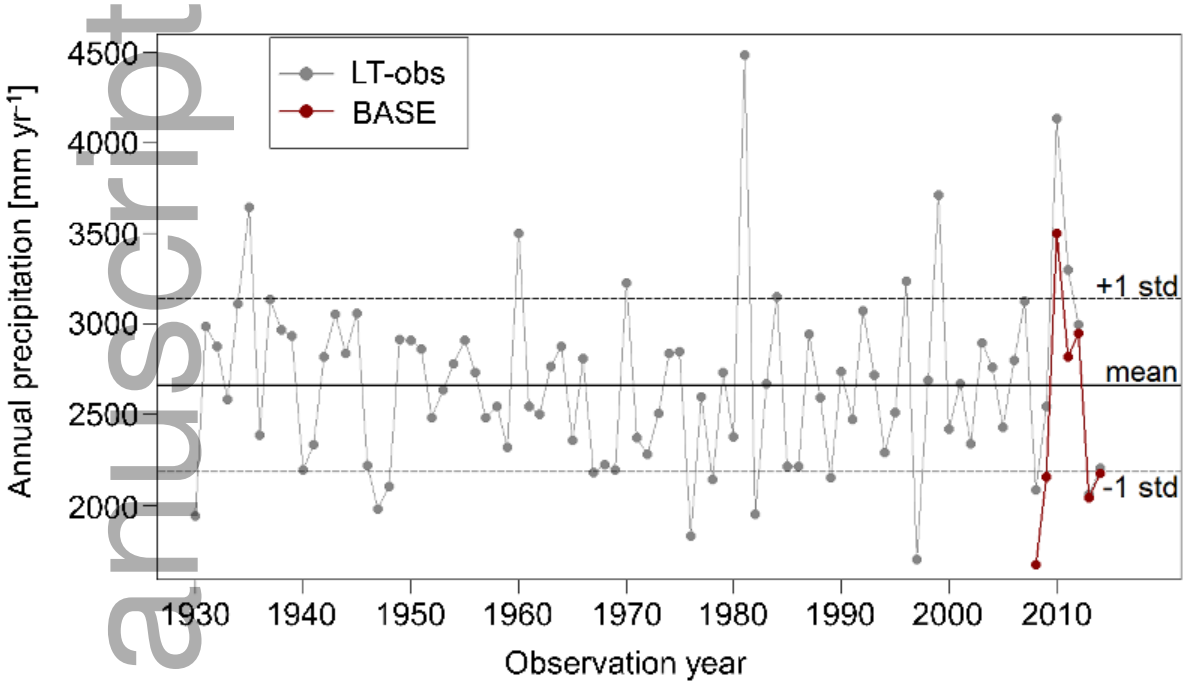

Fig. 1

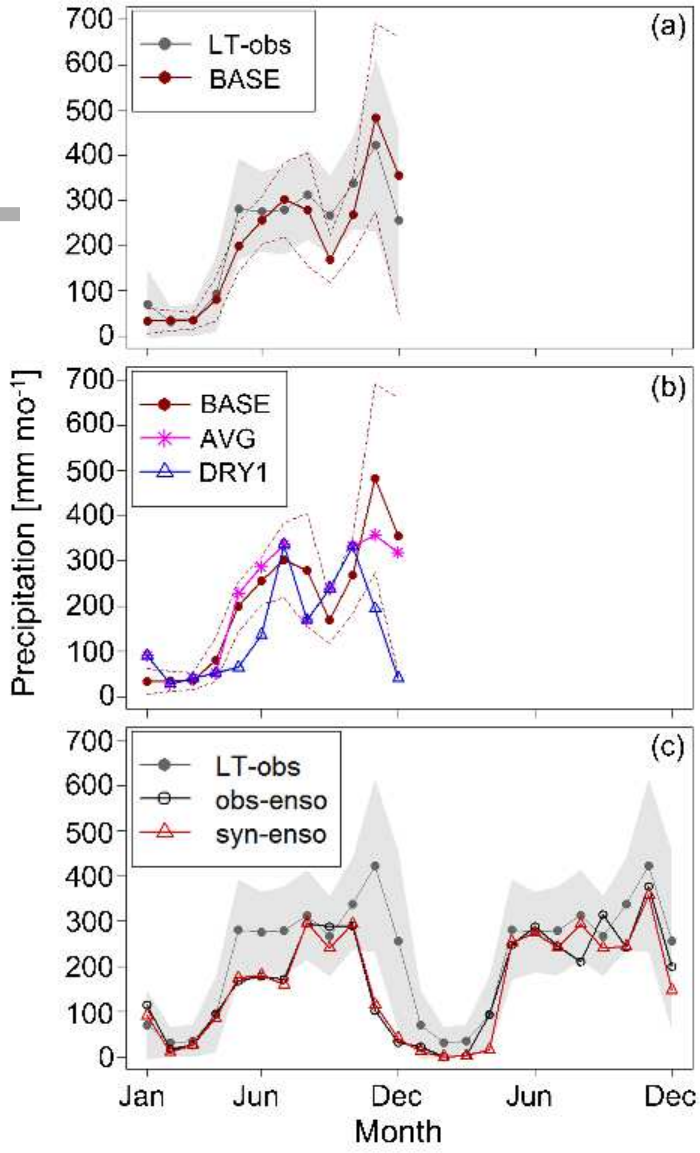

Fig. 2

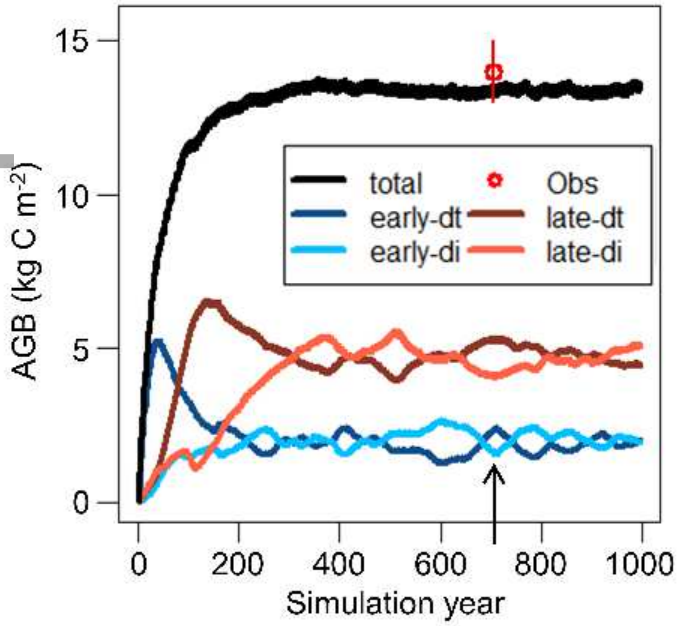

Fig. 3

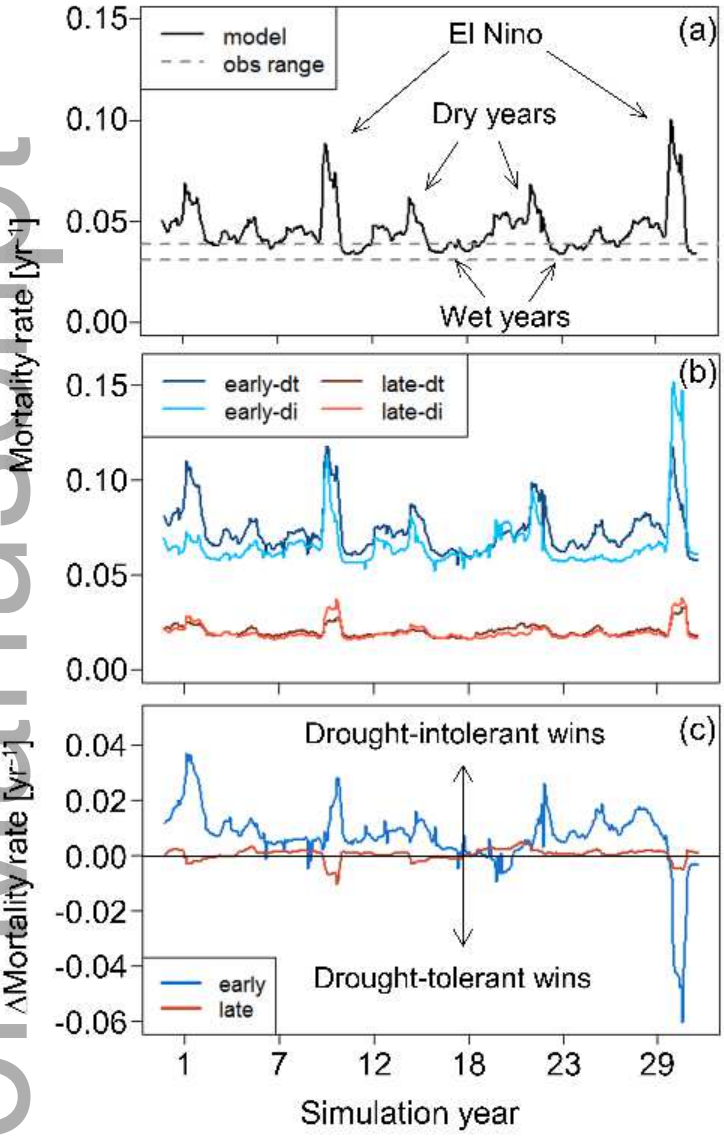

Fig. 4

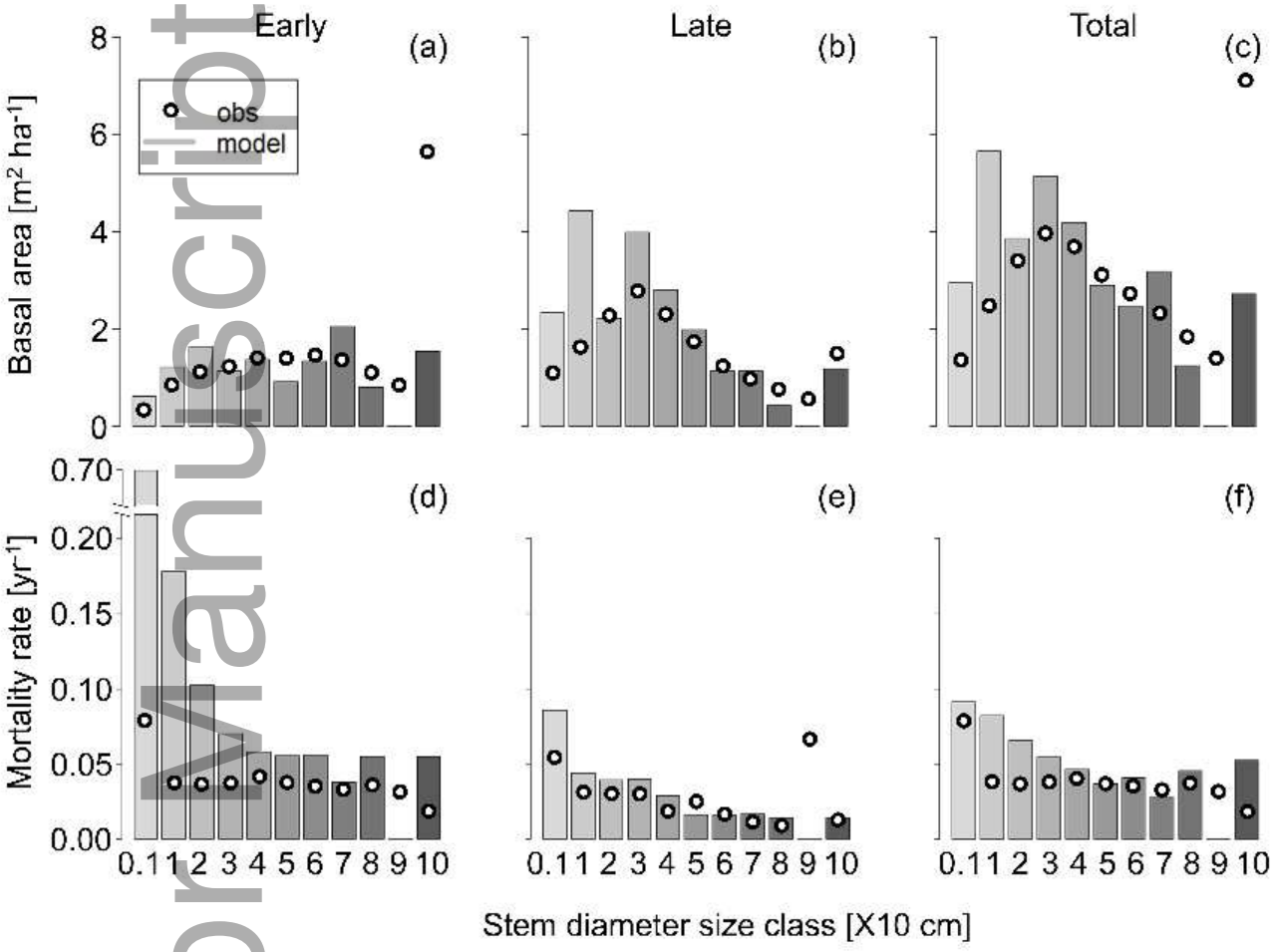

Fig. 5

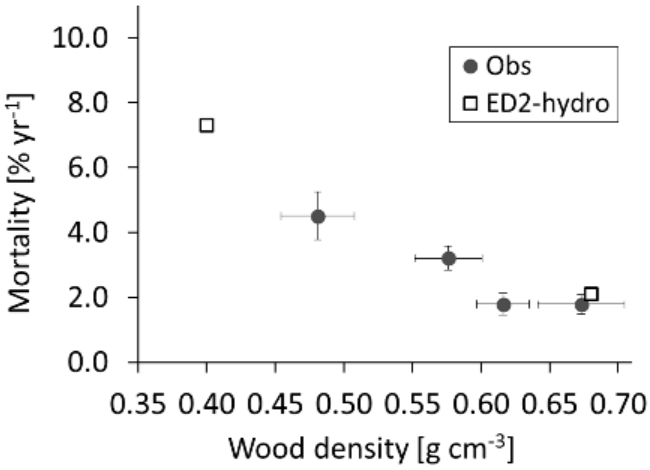

Fig. 6

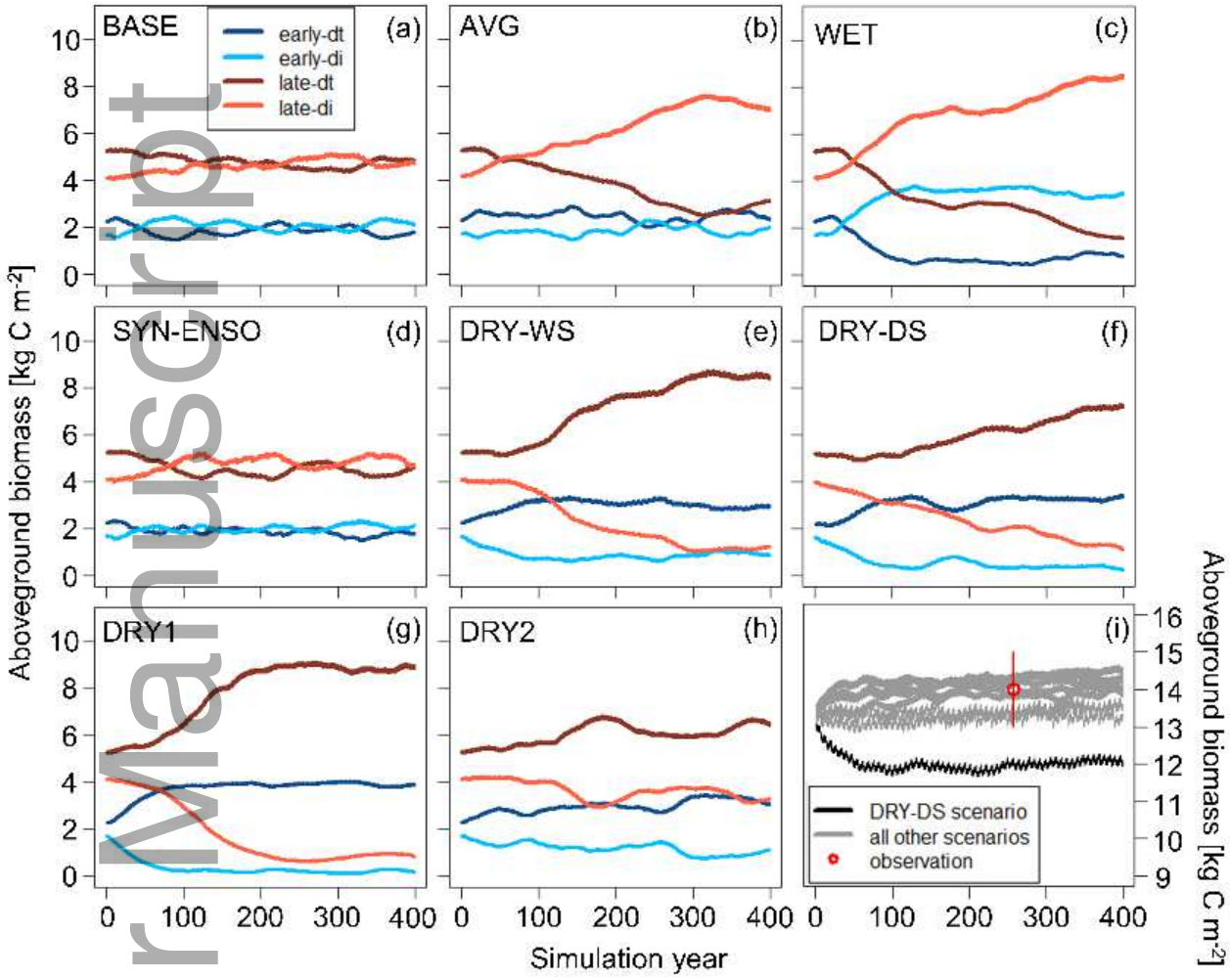

Fig. 7

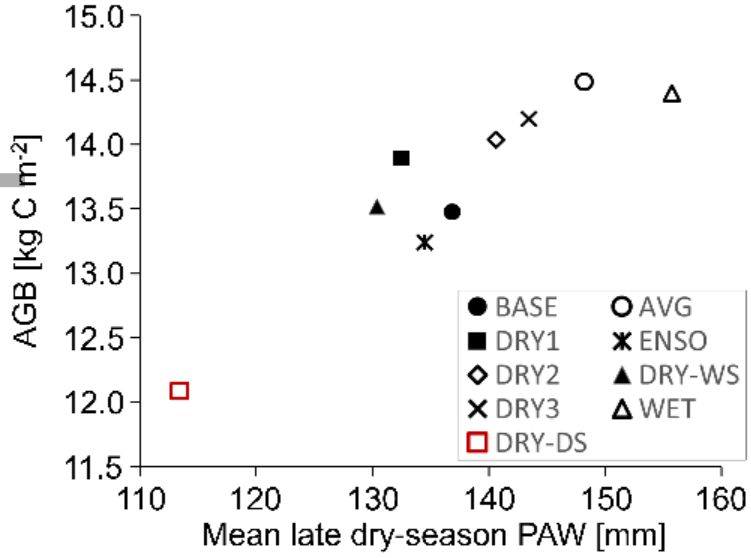

Fig. 8

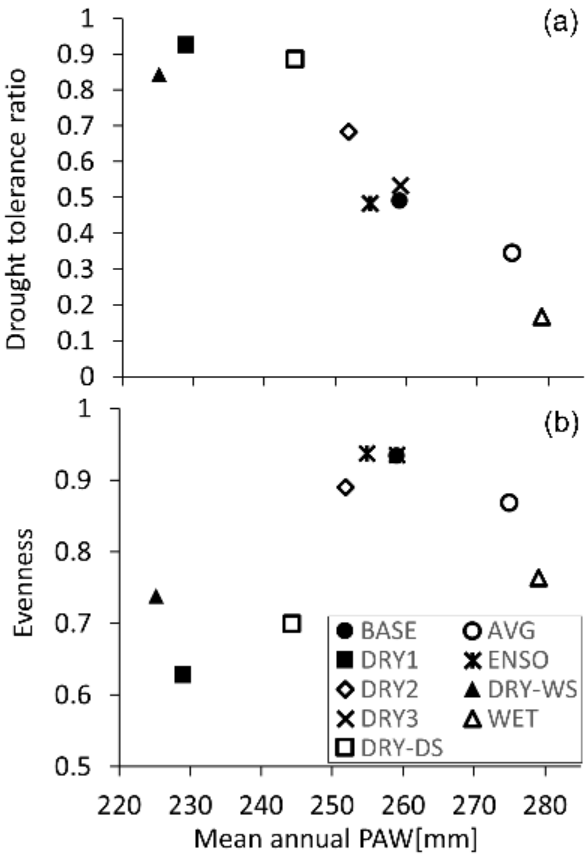

Fig. 9